Quasiresonant nonlinear optical processes involving excited and ionized atoms

S. M. Gladkov and N. I. Koroteev

M. V. Lomonosov State University, Moscow

Usp. Fiz. Nauk **160**, 105–145 (July 1990)

This review examines the nonlinear optical properties of highly excited and ionized gaseous media and low-temperature plasmas. The authors concentrate particularly on the role of excited atomic and ionized states, as well as continuum states. The authors cite and discuss experimental results of coherent anti-Stokes Raman scattering and optical harmonic generation in media consisting of excited atoms and ions. Nonlinear optical experiments involving the continuum states in intense optical fields are examined. In this connection the authors also discuss above-threshold ionization and the multiphoton stripping of atoms.

1. INTRODUCTION

Atoms are the traditional objects of study in nonlinear optics. Resonant nonlinear optical processes involving atoms have been widely investigated for the purposes of harmonic generation and other frequency conversion techniques,[1] as well as spectroscopic research, such as the measurement of oscillator strengths[2] and other atomic constants, etc. As a rule unexcited atoms were used in these investigations.

Currently, investigations of nonlinear optical properties of excited ions and atoms have attracted much interest. This interest has been motivated by the requirements of plasma spectroscopy on one hand and on the other hand by advances in the generation and application of extremely intense optical fields (high-power pico- and femtosecond pulses.)[3–6] Atoms placed in such intense fields undergo excitation and multiple ionization, and this markedly alters their original optical properties. Optical processes involving excited atomic states possess a number of interesting and practically important properties which will be discussed in this review. We will call these processes quasiresonant, since it turns out that even when no well-defined resonances exist between the radiation frequencies and the electronic transition frequencies, the efficiency of the processes is quite high and the polarization properties of scattered radiation turns out to be anomalous.

By varying the excitation level, the experimenter can "tune" the optical properties of the medium and shape them to the experimental requirements. This approach has proved particularly successful in solving practical problems.

In this review we shall examine the characteristic properties of coherent nonlinear scattering processes in highly excited gases, i.e., atomic and ionized gases. Obviously these coherent nonlinear scattering processes are closely related to their spontaneous analogs[7] and hence we cannot fail to touch upon spontaneous (noncoherent) light scattering processes in excited atomic and ionic gases as well.

Since this review shall address various light scattering processes, it is helpful to classify these processes and illustrate them with schematic transition diagrams, as shown in Fig. 1 (see Ref. 7). In spontaneous Raman scattering (SRS) the pump quanta are frequency-shifted towards the Raman-active transition frequency (see Fig. 1, a, b) and the emission quanta are noncoherent. Raleigh scattering (RS) corre-

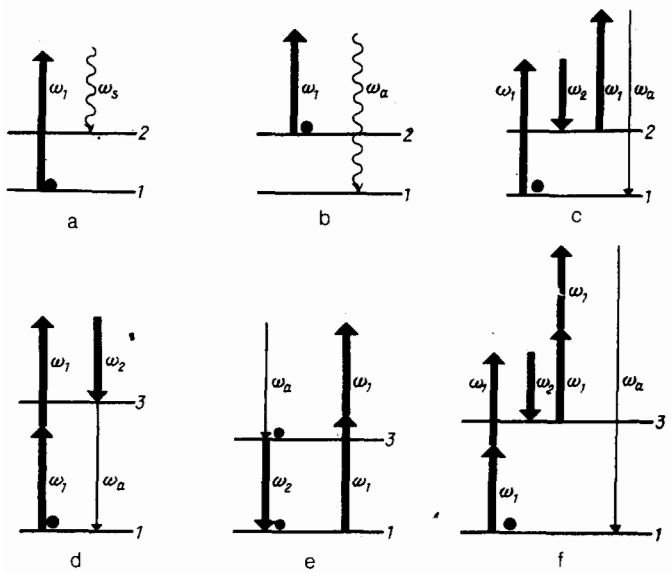

FIG. 1. Spectroscopic transition diagrams of various scattering processes discussed in this review. a–Stokes spontaneous Raman scattering (SRS); b–antiStokes SRS; c–coherent antiStokes Raman spectroscopy (CARS); d, e–degenerate active hyper-Raman spectroscopy (AHRS); f–nondegenerate AHRS. Circles indicate populated states.

 0038-5670/90/070554-22$01.00

sponds to the case where states 1 and 2 coincide. In Fig. 1, c we illustrate the coherent analog of spontaneous Raman scattering, known by the acronym CARS (coherent anti-Stokes Raman scattering). This process involves two pump frequencies ω_1 and ω_2. The scattered anti-Stokes radiation is coherent and quite intense compared to SRS radiation. Also in Fig. 1 we provide schematic diagrams of hyper-Raman scattering (HRS) in its four-photon (see Fig. 1, d, e) and six-photon variants (Fig. 1, f). (In Russian scientific literature the nomenclature of coherent anti-Stokes scattering comprises both CARS and four-photon HRS.) We shall examine the physical meaning of this terminology later in the review.

The contents of this review are organized as follows.

Section 2 introduces the concept of quasiresonance in the interaction of optical radiation with gases using the simplest models available: ensembles of noninteracting classical or quantum nonlinear oscillators.

In section 3 we examine Raleigh and spontaneous Raman scattering in atomic media. Simple estimates indicate that the crosssections of these processes increase significantly when the initial state is excited. We also discuss experimental results.

Section 4 is devoted to the nonlinear optical susceptibilities of excited atoms and ions. We discuss estimates of the cubic susceptibility of excited atomic hydrogen gas. We examine the transition from nonresonant to quasiresonant regime of interaction of light with a medium as the medium is excited, together with the related enhancement of nonlinear optical susceptibilities. We also discuss experimental results on coherent four-photon scattering in excited atomic and ionized media, i.e., active Raman and hyper-Raman scattering spectroscopy, and third harmonic generation.

Section 5 is devoted to quasiresonant coherent nonlinear optical processes in low-temperature, fairly dilute collisional gas plasma. In contrast to experiments in laser-assisted thermonuclear fusion, the experiments discussed here are not dominated by collective plasma nonlinearities. We also present simple models and experimental results.

Finally, in section 6 we analyze the features of harmonic generation in extremely intense light fields. We examine and classify experimental results obtained using subpicosecond laser pulses. We also propose several simple models to explain the experimental data. In these models the optically active electron is assumed to interact more strongly with the optical field than with the ion. Phase matching in strong fields is also discussed.

2. QUASIRESONANT LIGHT SCATTERING: SIMPLE MODELS

2.1. Excitation-induced intrinsic frequency lowering

Before proceeding with the discussion of nonlinear optical properties of real highly excited atoms and ions, let us consider two simple models of excited gaseous media to illustrate some general features of real nonlinear systems, both quantum and classical. These general features arise from a property common to many real physical systems possessing internal degrees of freedom: the tendency to become "soft" under excitation, that is to exhibit a lower intrinsic resonant frequency as the dissociation threshold is approached. As one excites an initially high-frequency system, it eventually becomes quasiresonant with the low-frequency external excitation, leading to enhanced linear and nonlinear optical susceptibilities of media composed of such systems.

2.2. Classical one-dimensional model

Classical models have been employed in nonlinear optics from the outset[11,12] to establish the general properties of nonlinear interaction between light and the medium. The earliest studies, however, examined only the simplest quadratic and cubic nonlinearities that are a priori relevant only at low excitation levels. As the excitation level increases, more complicated nonlinearities that can eventually lead to dissociation of the medium come into play.[9,10]

Consider two classical particles bound by a nonlinear force. In order to ensure harmonic oscillation at low amplitudes we require that the restoring force be "elastic", i.e., proportional to $-x$ (where x is the coordinate measured from the equilibrium position). Let the external field have the form $E_0 \sin(\omega t)$ (the spatial phase is immaterial in this example). When the response of the system, taking into account its initial excitation becomes sufficiently large this can result in dissociation of the real system. This requires that as $|x| \to \infty$ the restoring force tend to zero. An adequate model for systems bound by Coulomb-type forces is provided by a one-dimensional oscillator with a restoring force of the form:

$$F(x) = \frac{-x}{1+(x/a)^n},$$

where a is a constant. When $n = 3$ and $x \gg a$, $F(x)$ asymptotically reduces to the Coulomb interaction between two charges; $n = 4$ and $x \gg a$ corresponds to the interaction between a charge and a dipole, etc.

In the $n = 4$ case the corresponding potential is

$$V(x) = -\frac{a^2}{2}\left(\operatorname{arctg}\frac{x^2}{a^2} - \frac{\pi}{2}\right).$$

Clearly the parameter a reflects the half-width of the potential well. The equation of motion for such a system placed in an external field of amplitude E has the form:

$$x'' = -\frac{\omega_0^2 x}{1+(x/a)^4} + \frac{eE_0}{m}\sin(\omega t), \tag{1}$$

where each accent corresponds to a time derivative; m is the reduced mass; e is the charge; ω_0 is the frequency of intrinsic low-amplitude oscillations; ω is the external field frequency.

First consider the case of weak stimulated oscillations superposed on an initial background of sufficiently strong intrinsic oscillations of the system $x_0(t)$. This initial excitation (with the subsequent averaging over the initial phase) is analogous to the population of discrete energy levels in a quantum system. Let us also assume that the system is quite "hard" and the external field is low-frequency (a characteristic situation, for example, for Nd:YAG laser light scattering by hydrogen atoms). In other words, we take the following conditions to hold:

$$x_0 \gg x_E, \quad x_0 \gg a, \qquad E_0 \ll \frac{m\omega^2 x_0}{e}, \tag{2}$$

where $x_E(t)$ is the forced solution of equation (1); x_0 and x_E are the oscillation amplitudes.

In the first approximation, we can use a Taylor expansion of equation (1) to obtain

$$x_E^{\cdot\cdot(1)} = \frac{-\omega_0^2\{1-3[(x_0(t)+l)/a]^4\}x_E^{(1)}}{1+[(x_0(t)+l)/a]^4} + \frac{eE_0}{m}\sin(\omega t), \quad (3)$$

where, as mentioned earlier, $x_0(t)$ is the periodic "free" solution with a sufficiently large amplitude determined by initial conditions, and we have also introduced a constant displacement $l \gg x_0$ to make a series expansion possible for any moment in time. In the following discussion we shall omit this displacement from the formulae, but it is always implied. By averaging this expression over a time T ($\omega_0^{-1} \ll T \ll \omega^{-1}$) we immediately find that (3) becomes an equation for a linear harmonic oscillator with an intrinsic frequency ω' that is considerably lower than the low-amplitude oscillation frequency ω_0:

$$x_E^{\cdot\cdot} = -\omega'^2 x_E + \frac{eE_0}{m}\sin(\omega t), \quad (4)$$

$$\omega' = \omega_0 \frac{1}{T}\int_0^T \frac{1-3(x_0(t)/a)^4}{1+(x_0(t)/a)^4}\,dt \ll \omega_0.$$

Evidently the complex solution of equation (4) can be written as

$$x_E^{(1)} \sim \frac{1}{\omega'^2-\omega^2+i\gamma}.$$

Here we have introduced a phenomenological oscillator decay constant γ. Higher-order approximations can be obtained by a similar procedure. Thus we find that a highly excited nonlinear system can become quasiresonantly susceptible to an external low-frequency excitation at $\omega \approx \omega' \ll \omega_0$. This happens, for example, in systems near a phase transition that become unstable with respect to small perturbations. An optical example of this is the Rydberg atom.

In the quasiresonant regime, a medium composed of such classical nonlinear noninteracting oscillators exhibits enhanced linear and nonlinear light scattering (the phase matching conditions will be discussed in section 6).

2.3. Simple quantum picture

Consider a gaseous medium consisting of quantum particles with discrete energy levels labeled by the principal quantum number n. Suppose that for one reason or another (heating, electron collisions, etc.) some of the excited states are populated. As a result (see Fig. 2) linear and nonlinear optical processes will "start" from both the ground and the excited states. As a consequence of the rapid crowding of excited levels as one approaches the ionization threshold, characteristic for atoms and ions, transitions even between low-lying adjacent excited states have frequencies in the visible and near infrared ranges. These transitions accordingly become quasiresonant with the frequencies of the most common laser light sources. Moreover, as the principal quantum number n increases, the oscillator strength of transitions between adjacent levels ($\Delta n = 1$) increases as n^4 (until interactions between different particles become important, see section 3). Taken together, these factors lead to the quasiresonant enhancement of optical atomic characteristics such as polarizability (which increases as n^6), permittivity of the atomic medium as a whole, nonlinear susceptibilities, and so forth (see section 4 for details, also Refs. 13–15). The authors of Refs. 13, 14 have suggested that these effects can lead to self-focusing of the radiation.

3. RALEIGH AND SPONTANEOUS RAMAN SCATTERING IN EXCITED ATOMS

3.1. Permittivity of excited atomic and ionized media

Before evaluating the Rayleigh and spontaneous Raman scattering cross sections in excited atomic media, let us consider the behavior of the simplest optical parameter of a given medium–the permittivity $\varepsilon(\omega)$. If the quantum system has discrete energy levels, the permittivity can be written as

$$\varepsilon(\omega) = 1 + \frac{2N}{3\hbar}\sum_n\sum_i \frac{\rho_n\omega_{in}^2 |D_{ni}|^2}{\omega_{in}^2-\omega^2}$$

$$= 1 + \frac{4\pi e^2 N}{m}\sum_n\sum_i \frac{\rho_n f_{ni}}{\omega_{in}^2-\omega^2}, \quad (5)$$

where N is the particle number density; f_{ni} and D_{ni} are the oscillator strength and the matrix element of the dipole transition respectively. The summation runs over all discrete states with the principal quantum number n. For our purposes, the occupation ρ_n of the excited states can be assumed to obey the Boltzmann distribution

$$\rho_n = \frac{2n^2 g_n e^{-E_n/kT}}{\sum_n 2n^2 g_n e^{-E_n/kT}}; \quad (6)$$

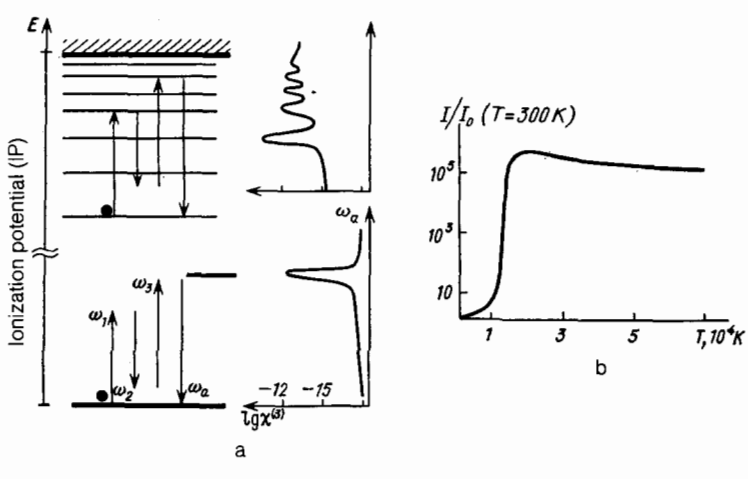

FIG. 2. Enhancement of cubic susceptibility $\chi^{(3)}$ due to excitation of an atomic gas (see Ref. 15) as an example of excitation-induced susceptibility enhancement. a–Transition diagram illustrating the quasiresonance between transitions in the medium and the external optical field. E is the energy of the state. b–Temperature dependence of the intensity I of the initially nonresonant CARS signal in a model atomic hydrogen gas (calculated in Ref. 15). I_0 is the scattering intensity at $T = 300$ K. Circles indicate populated states.

where kT is the temperature of the medium; E_n is the energy of the state; g_n are the statistical weight factors, which equal unity for free atoms. In the case of $\omega \ll \omega_{12}$, as the gas is heated it appears that $\varepsilon(\omega)$ should increase from unity to some peak value and then decay to less than unity. In fact this only happens when the frequency detuning between the radiation and one of the transitions does not exceed several hundred inverse centimeters. Otherwise the increase in $\varepsilon(\omega)$ due to the population of discrete levels is compensated by the negative free electron (plasma) component. In order to account for this additional component, another term of $-4\pi e^2 N_e/m\omega^2$ should be added to the right-hand side of equation (5), where N_e is the free electron concentration (see Ref. 14). As the heating increases, the gas becomes partially ionized and the magnitude of the plasma contribution grows rapidly. Therefore, given a large detuning, $\varepsilon(\omega)$ begins to decrease immediately upon heating. In order to confirm this prediction we can carry out a simple calculation for the case of atomic hydrogen gas. We calculate the permittivity $\varepsilon(\omega)$ taking into account the thermal population of discrete levels and the contribution of free electrons, while the fraction of ionized atoms is estimated from Saha's equation:

$$\frac{N_e^2}{N_a} = 4 \cdot \frac{2\pi mT}{\hbar^2} \frac{e^{-I/kT}}{Z}, \tag{7}$$

where N_{ae} are the concentrations of atoms and electrons respectively (these factors obey the sum rule $N_a + N_e = N_0$, in our estimates $N_0 = 2.7 \cdot 10^{19}$ cm^{-3}). The sum rule makes it possible to solve for N_e in equation (7). We also let I be the ionization potential of the hydrogen atom and Z be the partition function for the atom:

$$Z = \sum_n 2n^2 g_n e^{-E_n/kT}. \tag{8}$$

The weight factors g_n depend on the free electron concentration, falling between zero and one as a function of N_e. This dependence arises from the fact that microfields in the plasma "dissolve" the higher-lying discrete states and only the 3–4 lowest states of the hydrogen atom "survive" when N_e becomes of the order of 10^{18} cm^{-3} The calculation of g_n, is discussed in Ref. 16; in our estimates we have approximated the intensity distribution of the microfields by the Holtzmark function (see Ref. 17 for this and other definitions of the microfields). It suffices for our purposes to consider only the 15 lowest states of the H atom, since consideration of higher-lying states makes no appreciable difference to the results. The same technique for estimating the g_n factors was employed in calculating nonlinear susceptibilities.

Since equations (7) and (8) are mutually dependent, they are solved numerically by successive approximations. If in the first approximation g_n are all taken equal to unity, the solution usually requires 3–5 iterations. After calculating N_e and g_n self-consistently we can employ equation (5) to compute $\varepsilon(\omega)$. The calculated temperature dependence of $\varepsilon(\omega)$, including the plasma contribution, is shown in Fig. 3. Clearly this dependence varies with pump frequency: at $\omega = 15000$ cm^{-1} the quantity $(\varepsilon - 1)$ can increase significantly, while at $\omega = 17000$ cm^{-1} we find a monotonic decay. Thus we can conclude that the frequency spectrum contains quasiresonant bands several hundred or more cm^{-1} wide. The temperature limits of these bands depend on the detuning of the radiation frequency from the transitions in the medium. The quasiresonance occurs when the pump frequency falls into one of these bands and the medium is heated.

Not only does the linear atomic polarizability increase with excitation level, but so do the Rayleigh and spontaneous Raman scattering cross sections. Yet despite the large magnitudes of these cross sections (which can exceed 10^{-27} cm^2/sr, see below) the scattering signal is not easy to observe experimentally because of high levels of various masking signals due to recombination or bremsstrahlung that are invariably present in excited gases. This causes significant experimental difficulties.

In the following subsection we will discuss the calculation of RS and SRS, as well as the results of the relatively few experiments in this field.

3.2. Calculation of resonant Rayleigh and spontaneous Raman scattering cross-sections

The calculation of these cross-sections is relatively simple by virtue of the experimentally measured oscillator strengths of transitions between excited states. This approach was originally proposed and implemented by Penney.[18] First consider Rayleigh scattering. Let the scattering process start in a state with the quantum numbers T, J (the excited state will be labeled by T', J'). If $J = 0$ and the scattering particles are isotropic, the cross-section can be directly expressed in terms of the refraction index n_r ($\varepsilon(\omega) = n_r^2$).

$$(\sigma_{12})_{TJ \to TJ} = \frac{\omega^2}{c^4} \left(\frac{n^2 - 1}{4\pi N}\right)^2 \cos^2 \psi;$$

In the above expression Ψ is the angle between the unit vectors ε_1 and ε_2, where ε_1 defines the polarization orientation of the incident radiation and ε_2 is the direction onto which the scattered radiation is projected. If $J \neq 0$, the cross section formula is more cumbersome:

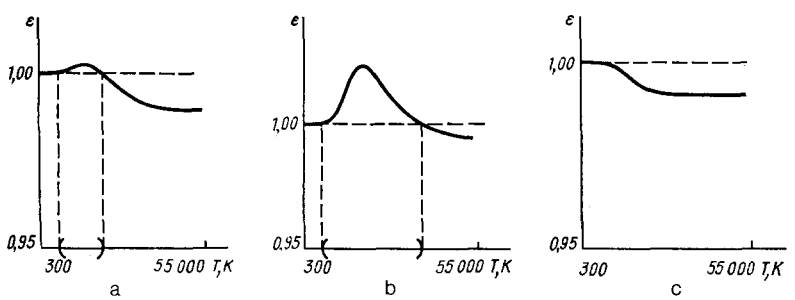

FIG. 3. Temperature dependence of the hydrogen gas permittivity ε at various frequencies (model calculation): a–$\omega = 14{,}000$ cm^{-1}; b–$\omega = 15{,}000$ cm^{-1}; c–$\omega = 17{,}000$ cm^{-1}. At $\omega = 17{,}000$ cm^{-1} the quasiresonance does not occur at any temperature. Brackets on the horizontal axis define the temperature limits of the quasi-resonance between the incident radiation and the $n = 2 \to n = 3$ transition.

$$(\sigma_{12})_{TJ\to TJ} = \sigma_{zz}\cos^2\psi + \sigma_{zx}\sin^2\psi,$$

where

$$\sigma_{zz} = 9(2J+1)\omega^4\frac{e^2}{mc^2}\sum_M \times\left[\sum_{T'J'}\frac{f_{TJ,T'J'}}{\omega^2_{T'J',TJ}-\omega^2}\begin{pmatrix} J' & 1 & J \\ -M & 0 & M\end{pmatrix}\right]^2,$$

$$\sigma_{zx} = \frac{9}{4}(2J+1)\omega^4\frac{e^2}{mc^2}\sum_M\left\{\sum_{T'J'}\frac{f_{TJ,T'J'}}{\omega^2_{T'J',TJ}} \times\left[\frac{\begin{pmatrix} J' & 1 & J \\ -M & 0 & M-1\end{pmatrix}\begin{pmatrix} J' & 1 & J \\ -M & 0 & M\end{pmatrix}}{\omega_{T'J',TJ}-\omega} + \frac{\begin{pmatrix} J' & 1 & J \\ -M+1 & 0 & M-1\end{pmatrix}\begin{pmatrix} J' & 1 & J \\ -M+1 & 0 & M\end{pmatrix}}{\omega_{T'J',TJ}+\omega}\right]^2\right\},$$

here the quantities in round brackets are the $3J$ symbols. Consequently, when the scattering "starts" from a state with $J \neq 0$, the scattered light is depolarized. Recently this fact was experimentally verified in excited barium ions.[19]

In spontaneous Raman scattering, the scattering cross-sections for processes involving many intermediate states were first calculated in terms of oscillator strengths by Vriens.[20] The result was as follows

$$(\sigma_{zb})_{TJ\to T'J'} = \frac{(\omega-\omega_{T'J',TJ})^4 e^4}{\hbar^2 c^4(2J+1)}\sum_M \times\left|\sum_{T''J''}\langle T''J''|D|T'J'\rangle^*\langle T''J''|D|TJ\rangle \times\left[\frac{\begin{pmatrix} J' & 1 & J'' \\ -M' & q & M\end{pmatrix}\begin{pmatrix} J'' & 1 & J \\ -M & 0 & M\end{pmatrix}}{\omega_{T''J'',TJ}-\omega} + (-1)^q\frac{\begin{pmatrix} J' & 1 & J'' \\ -M' & 0 & M'\end{pmatrix}\begin{pmatrix} J' & 1 & J \\ -M' & q & M\end{pmatrix}}{\omega_{T''J'',T'J'}+\omega}\right]\right|^2,$$

here the Raman transition is the $TJ \to T'J'$ transition; $b = z$ and $q = 0$ for polarized scattering, and $b = x$ and $q = 1$ for depolarized scattering. The quantities in the angle brackets are the reduced dipole moment matrix elements, which can be expressed in terms of the oscillator strengths f for the appropriate transitions:

$$\langle T''J''|D|T'J'\rangle^*\langle T''J''|D|TJ\rangle = \frac{3\hbar\xi(T''J'')}{m}\left|\frac{2f_{TJ,T''J''}f_{T'J',T''J''}}{\omega_{T''J'',TJ}\omega_{T''J'',T'J'}}\right|^{1/2}, \quad (9)$$

where ξ can be $+1$ or -1 depending on the type of transition. Information on the oscillator strengths is tabulated in reference handbooks of Ref. 21, 22, but the signs of the matrix elements, i.e., the sign of ξ, cannot be obtained from these tables. They can be determined by direct calculation (which need only be sufficiently accurate to determine the sign of the matrix element, rather than the actual value). A detailed discussion of this problem is available in Refs. 23, 128. The correct assignment of the sign can be verified by comparing the experimentally measured depolarization coefficient $\rho = \sigma_{zx}/\sigma_{zz}$ with the calculated value. This verification was carried out for some atoms by Vriens,[20] who also calculated the SRS cross sections for various excitation wavelengths using the above formula. For example, for Stokes scattering (starting from the ground state $^2P_{1/2}$) at $\lambda = 6943$ Å in indium atoms In $\sigma_{zz} = 0.68\cdot10^{-27}$ cm^2/sr and $\rho = 0.68$; at the same λ in thallium be found Tl $\sigma_{zz} = 5.5\cdot10^{-29}$ cm^2/sr and $\rho = 0.76$. Somewhat different values were obtained for the antiStokes scattering (starting from the excited state $^2P_{3/2}$): at the same wavelength In $\sigma_{zz} = 1.6\cdot10^{-27}$ cm^2/sr and $\rho = 0.78$; Tl $\sigma_{zz} = 15.9\cdot10^{-29}$ cm^2/sr and $\rho = 0.83$. Note that the scattering cross sections and depolarization coefficients are significantly higher when the scattering starts from an excited state. This enhancement is not so much due to the ω^2 factor as to the diminution of the resonant terms in the denominators of the cross-section formula. This tendency was convincingly confirmed by Vriens and Adriaansz,[24] who calculated the Rayleigh and spontaneous Raman scattering cross sections starting from higher-lying states of neon, argon, and xenon atoms. The results for linearly polarized radiation at $\lambda = 6943$ Å are summarized in Table I.

Clearly, starting from higher-lying states strongly enhances both the RS and SRS cross sections compared to starting from the ground state. This is largely due to the diminution of the frequency-dependent denominators in the cross section formula because of the crowding of excited levels (see also Fig. 2). The cross section enhancement is so strong that the population of even a small number of excited states markedly increases the scattered signal intensity. Nonetheless, because of the above-discussed reasons, in electric discharge conditions the SRS process starting from excited levels has only been observed in one experiment,[24]

TABLE I.

Atom	Initial state	Final State	σ_{zz}, cm^2/sr	ρ	Scattering process
Ne	$2p^6$ [0] (ground state)	$2p^6$ [0]	$1.03\cdot10^{-29}$	0	Rayleigh
	$1s_2$ [1]	$1s_2$ [1]	$2.76\cdot10^{-22}$	0.381	»
	$1s_2$ [1]	$1s_4$ [1]	$8.09\cdot10^{-23}$	—	Raman
Ar	$3p^6$ [0] (ground state)	$3p^6$ [0]	$1.81\cdot10^{-28}$	0	Rayleigh
	$1s_5$ [2]	$1s_5$ [2]	$1.73\cdot10^{-24}$	0.975	»
	$1s_5$ [2]	$1s_3$ [0]	$4.42\cdot10^{-24}$	—	Raman

where a special effort was made to reduce background signals.

Let us briefly touch on the estimated contribution of the continuum (bound state–continuum transitions) to the cross section. It turns out that both for unexcited free atoms[25] and excited atoms[26] the continuum contributes no more than 10%. In the case of atoms in a plasma one should either apply the theory developed for two-photon transitions in a screened Coulomb potential (see Ref. 27 and references therein) or employ empirical photorecombination data.

3.3. Spontaneous Raman scattering involving fine-structure atomic states

The most promising transitions for observing Raman scattering in atoms are those between the fine structure of the ground state created by the spin-orbit interaction. The total angular momentum of adjacent states differs by unity and all states belonging to the same spin-orbit multiplet have the same parity. Transitions with $|\Delta J = 1|$ are magnetic dipole transitions (with possible quadrupole contributions), while transitions with $|\Delta J = 2|$ are pure quadrupole. Absorption and emission transitions between such states are forbidden in the dipole approximation and hence Raman scattering is the appropriate spectroscopic technique.

In metallic atoms that have low-lying electronic states, even scattering processes that start from the ground state are quasiresonant. The SRS cross section in this case usually falls in the 10^{-27}–10^{-22} cm^2/sr range, much larger than the corresponding quantity in molecules (usually of the order of 10^{-31} cm^2/sr). In atoms that have no low-lying electronic states, transitions that have a large oscillator strength and involve the ground state have rather low cross sections: for instance, the $^2P_{3/2} \rightarrow {}^2P_{1/2}$ transition in fluorine atoms has a cross section of the order of $2 \cdot 10^{-31}$ cm^2/sr.[28]

Today, experiments on spontaneous Raman scattering in atoms no longer appear esoteric. Nonetheless, not many such experiments (of the order of ten) have been performed to date.[28–36] A concise review is available in Ref. 37. Most of these experiments employed atomic media prepared by thermal heating. In nonequilibrium and plasma media no experiments have been attempted because of the weakness of scattered signal compared to the background (with the exception of the one above-discussed experiment).[24]

4. NONLINEAR OPTICAL SUSCEPTIBILITIES OF EXCITED ATOMS AND IONS

4.1. A new phase in studies of optical nonlinearities in excited media

There are a number of reasons for the current interest in the nonlinear optical properties of excited atomic and ionized media. As we have mentioned in the introduction, such research is essential for a true understanding of interactions between superintense optical fields and gaseous media; for the development of new methods in plasma spectroscopy; and for the measurement of nonlinear susceptibilities of atoms and ions, which represent new and independent combinations of atomic and ionic parameters. First we will consider the lowest order nonlinear susceptibilities which correspond to four-photon processes, since in isotropic gaseous media quadratic nonlinearities cancel to zero (second harmonic generation mechanisms are discussed in Ref. 83). These processes include coherent antiStokes Raman scattering (CARS)[7] and third harmonic generation (THG). Four-photon processes were extensively studied in unexcited atomic media for the purposes of optical frequency conversion (for a review see, for example, Ref. 1). We shall focus our attention on the properties of such processes involving excited atoms and ions.

The first indications of nonlinear susceptibility enhancement due to the population of excited discrete states in gaseous media were reported in Refs. 13, 14.

As will become clear later, nonlinear susceptibility enhancement increases with the order of the nonlinear process (in powers of the exciting field). This makes it possible to investigate scattering processes that are difficult to observe in unexcited gaseous media.

4.2. Quasiresonant enhancement of nonlinear susceptibilities

A general expression for the cubic susceptibility tensor $\chi^{(3)}$ of an atomic gas was derived by Yuratich and Hanna:[38]

$$\chi^{(3)}(\omega_0;\ \omega_1,\ \omega_2,\ \omega_3) \propto \mathrm{St} \sum_{\substack{n,J\\ n_1,J_1,\\ n_2,J_2,\\ n_3,J_3}} \sum_{k=0}^{2} (-1)^{3J+J_3+k} \rho^{(0)}_{nJ,nJ} \frac{(2k+1)^{1/2}}{2J+1}$$
$$\times \langle nJ|D|n_1J_1\rangle \langle n_1J_1|D|n_2J_2\rangle \langle n_2J_2|D|n_3J_3\rangle \langle n_3J_3|D|nJ\rangle$$
$$\times \begin{Bmatrix} J & k & J_2 \\ 1 & J_1 & 1 \end{Bmatrix} \begin{Bmatrix} J & 1 & J_3 \\ 1 & J_2 & k \end{Bmatrix} \frac{(((\varepsilon_0\varepsilon_1)^{(k)}\varepsilon_2)^{(1)}\varepsilon_3)^{(0)}_0}{D_\omega(nJ,\ n_1J_1,\ n_2J_2,\ n_3J_3;\ \omega_1\omega_2\omega_3)}; \qquad (10)$$

where n and J are quantum numbers; ε_0 and ε_1 are the unit polarization vectors of the scattered signal and the pump; $\langle nJ|D|nJ\rangle$ are the reduced dipole moment matrix elements expressed in terms of oscillator strengths of the appropriate transitions [see formula (9)]; St is the operator of all possible interchanges of frequency subscripts. The frequency denominators D_ω (there are 48 of them in the most general case) contain all the possible resonances–they are enumerated explicitly in Ref. 39. The above formula takes into account all processes that start from excited states whose population $\rho^{(0)}_{nJ,nJ}$ can be estimated from the Boltzmann formula [see formula (6)].

At sufficiently high temperatures some of the atoms are ionized. The fraction of ionized atoms can be computed from the Saha formula (see section 3). Expression (10) does not include the contribution of continuum states; their importance to accurate calculations for free atomic media was demonstrated by Manakov and co-workers.[40] At sufficiently high pressures or at temperatures reaching tens of thousands of degrees, the higher-lying discrete states and the adjacent continuum states are washed out (see subsection 3.1) and the approach developed in Ref. 40 becomes invalid. In this situation the contribution of free electron plasma to the scattering must be calculated by a different technique (see below, section 5). Nonetheless, formula (10) is valid for qualitative estimates, since even a small density of excited discrete states can play a significant role in the quasiresonant regime. In the particular case of the hydrogen atom the reduced dipole moment matrix elements are known[41] and their sign does not pose a problem[23] since the radial integrals are positive for all nondegenerate transitions.

Returning to Fig. 2, we can analyze expression (10) to verify that the efficiency of both resonant and "non-reso-

nant" (i.e., not in precise resonance with some atomic transition) processes is greatly enhanced as excited states are populated. As it happens, frequencies in the visible and near infrared ranges become quasiresonant with electronic transitions in excited gaseous media. By virtue of the rapid diminution of the frequency denominators D_ω the cubic susceptibility can gain several orders of magnitude as the gas is excited, i.e., far outweigh the linear susceptibility enhancement $[\varepsilon(\omega)-1]/4\pi$ (see subsection 3.1). The frequency limits of quasiresonant bands widen correspondingly. The increasing oscillator strengths for transitions between adjacent states that accompany the growth of principal quantum number n can also contribute to the susceptibility enhancement, although here we should also take into account the broadening of excited states by plasma microfields (see subsection 3.1).

We have applied expression (10) to estimate the cubic susceptibility $\chi^{(3)}$ of CARS processes in a model gas consisting of hydrogen atoms excited by an equilibrium heating.[15,42] If the CARS process starts from the ground state of the H atom, it remains nonresonant for all pump frequencies in the visible range. However, the population of even a small number of excited states renders the process quasiresonant. The susceptibility can increase over its nonresonant value by several orders of magnitude without exhibiting any well-defined frequency dependence that is characteristic of resonant processes. We emphasize again that in real, dense, partially ionized gaseous media the highly excited atomic states and the adjacent continuum states are markedly different from their counterparts in free atoms:[16] the Rydberg states are washed out by plasma microfields and the oscillator strength increases with principal quantum number only up to a point, decaying rapidly thereafter. A proper treatment of such systems requires either a semi-empirical approach or a rigorous statistical theory of nonlinear optical processes in a plasma that takes into account the microstructure of the plasma particles.

The results of our calculations of the cubic susceptibility $\chi^{(3)}(\omega_0;\ \omega_1,\ \omega_1,\ -\omega_2)$ of a model atomic hydrogen gas[15-42] are shown in Fig. 3. When the gas is heated to $T\approx 10^4$ K the quantity $|\chi^{(3)}|^2$, proportional to the scattered signal intensity, increases by an order of magnitude; at $T\approx(3\text{–}5)\cdot 10^4$ K the intensity enhancement would reach 5–6 orders of magnitude, but at such high temperatures the free electron contribution can no longer be neglected. Nonetheless, the trend is clear: the initially nonresonant CARS process becomes quasiresonant as the medium is excited, with the attendant strong enhancement of signal intensity. This conclusion is indirectly corroborated by CARS experiments in low-temperature laser plasmas (see below, section 5). We should also mention in this connection that as the nonlinearity order in powers of the exciting field increases, so does the number of frequency denominators. Hence the relative scattering enhancement increases as well. This holds out the hope of observing in excited media scattering processes that are too weak in unexcited gases.

4.3. Polarization anomalies in CARS processes starting from excited states

Not only do four-photon light scattering processes exhibit enhanced efficiencies in excited atoms and ions, but the scattered signal also has anomalous polarization properties. Polarization analysis is frequently employed in CARS spectroscopy,[7,43] providing another diagnostic "degree of freedom". In excited media CARS processes characteristically exhibit quasiresonance-induced "polarization anomalies" in the scattered signal.

Let us address this point in more detail by examining a CARS process based on Raman scattering (Fig. 4). In the case of a partially degenerate process ($\omega_a = 2\omega_1 - \omega_2$), the vector $\mathbf{P}_{CARS}$ which fixes the **E** vector orientation of the scattered signal can be expressed as[43]

$$\mathbf{P}_{\text{KAPC}} = 2\chi_{1122}\mathbf{e}(\mathbf{e}_1\mathbf{e}_2) + \chi_{1221}\mathbf{e}_2(\mathbf{e}_1\mathbf{e}_1),$$

where $\mathbf{e}_i$ are the unit vectors corresponding to the $\mathbf{E}_i$ vectors of the linearly polarized pump beams; χ_{1122} and χ_{1221} are the linearly independent components of the $\chi^{(3)}$ tensor. The components of the $\mathbf{P}_{CARS}$ vector projected onto the unit vectors $\mathbf{e}_1$ and $\mathbf{e}_2$ (in experiments these are usually separated by an angle $\varphi\approx 70°$) are, respectively,

$$(\mathbf{P}_{\text{KAPC}})_1 = 2\chi_{1122}\cos\varphi, \qquad (\mathbf{P}_{\text{KAPC}})_2 = \chi_{1221}.$$

As long as we are far from single-photon resonances, the following relations are valid for the Raman-based CARS process:

$$\chi_{1122} \sim -\gamma_1 + \gamma_2, \qquad (11)$$
$$\chi_{1221} \sim \gamma_1 + \gamma_2,$$

where γ_1 and γ_2 are the antisymmetric and anisotropic invariants of the Raman scattering tensor.[44] Taken separately, the tensor invariants–γ_0 (isotropic), γ_1, and γ_2–produce respectively isotropic, antisymmetric, and anisotropic components of the $\mathbf{P}_{CARS}$ vector (see Fig. 4, c):

$$\mathbf{P}_{is} \sim 3\mathbf{e}_1\cos\varphi;$$
$$\mathbf{P}_{anti} \sim \mathbf{e}_1\cos\varphi - \mathbf{e}_2,$$
$$\mathbf{P}_{anis} \sim \mathbf{e}_1\cos\varphi + 3\mathbf{e}_2.$$

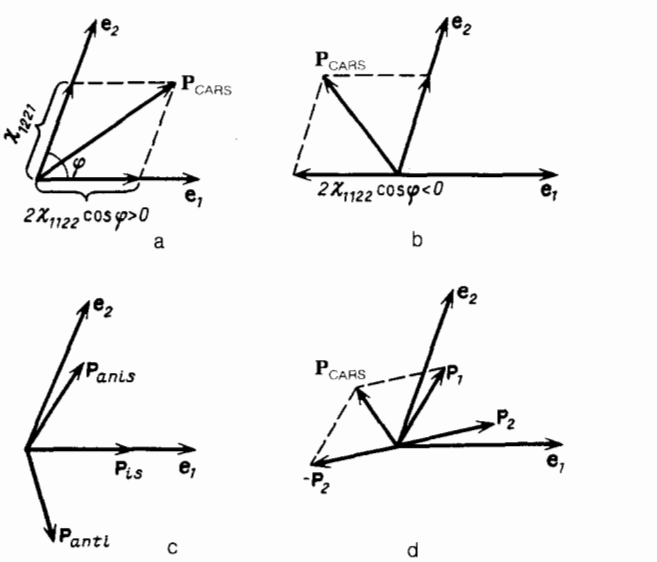

FIG. 4. Polarization of the CARS signal from a Raman resonance. $\mathbf{e}_1$ and $\mathbf{e}_2$ are the polarization unit vectors of the linearly polarized pump beams, $\mathbf{P}_{CARS}$ is the polarization vector of the scattered signal. a–ordinary "nonresonant" polarization (cold gas); b–anomalous polarization in the quasiresonant regime; c–contributions of different scattering tensor invariants to $\mathbf{P}_{CARS}$; d–contributions of various excited states that interfere to produce the anomalous polarization of $\mathbf{P}_{CARS}$ signal.

Far from single-photon resonances the antisymmetric invariant γ_1 is small.[44] The Raman-based $\mathbf{P}_{CARS}$ vector becomes a linear combination of isotropic and anisotropic components and therefore lies between $\mathbf{e}_1$ and $\mathbf{e}_2$. If the process approaches a single-photon resonance invariant γ_1 increases and the χ_{1122} can become negative–the $\mathbf{P}_{CARS}$ vector can then fall outside the sector delimited by $\mathbf{e}_1$ and $\mathbf{e}_2$. We shall term this polarization state anomalous because it never occurs in classical CARS spectroscopy of unexcited molecular media. Here we note that the above analysis of the polarization state is not rigorously valid, since in the vicinity of single-photon resonances relations (11) may no longer apply.[7] Nonetheless this type of analysis is instructive in pointing out the reason behind polarization anomalies: the quasiresonance between the pump frequencies and transitions in the medium. The above-discussed model computation for the atomic hydrogen gas (Fig. 5) leads to the same conclusion as our qualitative argument. As the gas is heated the $\mathbf{P}_{CARS}$ vector rotates into the anomalous position.

Polarization anomalies can also result from the interference between the contributions of various excited states to $\chi^{(3)}$. For example, if two states produce $\mathbf{P}_{CARS}$ vectors that point in the "normal" direction (between $\mathbf{e}_1$ and $\mathbf{e}_2$) but have opposite signs, the total polarization can become anomalous (see Fig. 4, d). We note that this mechanism is based on nothing else but the discreteness of the energy spectrum of the scattering particle.

4.4. Active Raman spectroscopy of fine-structure atomic states

In this subsection we will discuss experimental results of CARS spectroscopy based on Raman scattering involving atomic fine-structure states. A reasonably complete bibliography of this field is available in several review articles.[37,48,47] We shall briefly examine the appropriate experimental techniques and the main results obtained in this new branch of CARS spectroscopy.

It is well known that CARS is the coherent analog of spontaneous Raman scattering (SRS).[7] The cubic susceptibility for this process can be simply expressed in terms of SRS cross section (away from single-photon resonances):

$$\chi^{(3)} \approx \frac{Nc^4}{24\hbar\Gamma\omega^4}\sigma_{CKP},$$

where N is the density of scattering particles; Γ is the half-width of the Raman resonance. In quasiresonant conditions both σ_{SRS} and $\chi^{(3)}$ increase simultaneously. Since CARS is a coherent process the scattered signal is quite intense and has all the properties of laser radiation. Consequently, the CARS process is experimentally more accessible than SRS, at least in reasonably dense media.

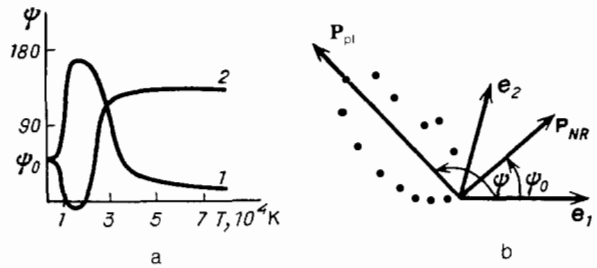

FIG. 5. Calculated and experimental orientations of the $\mathbf{P}_{CARS}$ vector in excited gas. a–calculated temperature dependence of the rotation angle Ψ of the $\mathbf{P}_{CARS}$ vector: curve *1* corresponds to pump frequencies $\omega_1/2\pi c$ and $\omega_2/2\pi c$ of 16,000 and 15,000 cm^{-1} respectively, curve *2* corresponds to $\omega_1/2\pi c = 17{,}000\ cm^{-1}$ and $\omega_2/2\pi c = 16{,}000\ cm^{-1}$. b–orientation of the $\mathbf{P}_{pl}$ vector of the quasiresonant antiStokes signal in optical breakdown plasma (experimental data from Ref. 45). The experimental data are shown as points on a polar diagram. $\mathbf{P}_{NR}$ corresponds to scattering in "cold" gas; $\Psi_0 = 43°$.

Consider the typical experimental setup for four-photon spectroscopy of excited gases (Fig. 6). It consists of a pulsed CARS spectrometer based on Nd:YAG crystals operated in the Q-switched regime: the optical pulse duration is approximately 15 ns, the repetition rate is 10–15 Hz. After its generation, radiation at $\lambda = 1.06\ \mu m$ is amplified in two independent channels using Nd:YAG crystals and then frequency-doubled using CDA crystals. The second harmonic ω_1 from one of the channels is used to pump a frequency-tunable (ω_2) dye laser. As a result the radiation energy reaches 50 mJ at frequency ω_1 ($\lambda = 0.53\ \mu m$) and 2 mJ at frequency ω_2. Dichroic mirrors are employed to make the beams perfectly collinear, while telescopes T equalize the beam diameters and divergences. Finally, the two beams are focused into a cell containing the gas. Both narrow-band and wide-band CARS variants can be used.[7] After filtering with optical filters and optical scanning with a polychromator, the optical signal at frequency ω_a is detected by an optical multichannel analyzer (OMA) connected to a personal computer.

Atomization and excitation of gaseous media is accomplished by several methods. Volatile metallic vapors are produced by thermal heating in a quartz cell. Also, arc and spark discharge excitation is utilized via optical breakdown

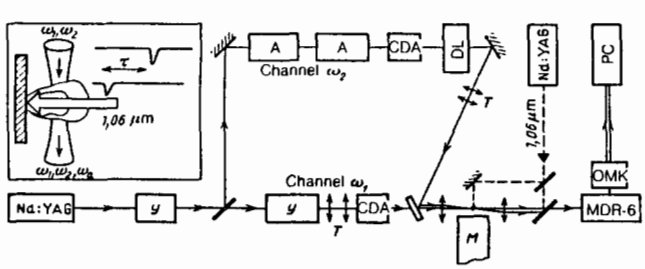

FIG. 6. Experimental arrangement for four-photon spectroscopy of atoms and ions. Nd:YAG is the source of radiation at $\lambda = 1.06\ \mu m$ based on neodimium-doped yittrium–aluminum garnet crystals; A –amplifiers based on Nd:YAG crystals; CDA–frequency doublers based on CDA crystals; DL–organic dye laser; T–telescopes for adjusting beam diameters and divergences; M–metallic target; PC–personal computer; OMA–optical multichannel analyzer; MDR-6–polychromator. Inset on the left illustrates nonlinear optical probing of the optical breakdown region; τ is the time delay between the excitation and probe pulses.

or selective optical population. The optical breakdown can be engineered by an additional nanosecond pulsed (Nd:YAG) system synchronized with the CARS spectrometer (see Fig. 6). Breakdown is achieved either by focusing the radiation directly into the gas or onto the surface of a metallic target. By this technique one can prepare densities of excited atoms of nonvolatile metals reaching 10^{19} cm^{-3}. The delay between the CARS probe pulse and the excitation pulse of electric or optical breakdown can be varied in a wide range: between 50 ns and 100 μs.

Only a few active CARS spectroscopy experiments have been performed on atoms to date,[48-53] probably because this type of spectroscopy has traditionally been concerned with other media and also because of purely technical difficulties. Yet these experiments are obviously promising: in addition to studying the Raman-active transitions in strongly luminescent atomic media (which is not possible with SRS) and the kinetics of the corresponding states (including metastable ones), one can populate excited states corresponding to magnetic dipole and quadrupole transitions; and also measure the cubic susceptibility components, compare them with calculated results, and extract information on the signs of the reduced matrix elements (to take one example). Active Raman spectroscopy can be employed in the diagnostics of lasers based on the fine structure of the electronic ground state of halogen atoms, like the iodine laser.

The first experimental study of CARS in atoms apparently was carried out by Teets and Bechtel in 1981.[48] They studied CARS in oxygen atoms produced in the flame of an oxygen-hydrogen burner at approximately 3000 K. A diagram of the lower-lying O atom states (spin-orbit triplet) is shown in Fig. 7. The transitions between adjacent states ($|\Delta J| = 1$) that have the same parity are either magnetic dipole or quadrupole (when $|\Delta J| = 2$ they are pure quadrupole). When the frequency difference $\omega_1 - \omega_2$ coincides with transition frequencies $^3P_0$–$^3P_2$ or $^3P_0$–$^3P_1$ (which are 227 and 158 cm^{-1} respectively), the CARS spectrum exhib-

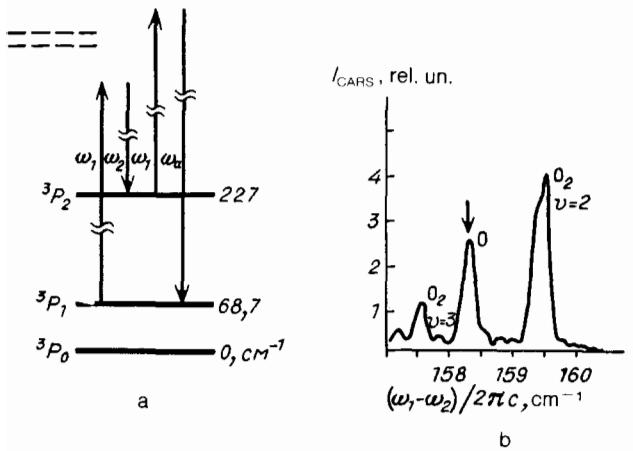

FIG. 7. Coherent antiStokes scattering in oxygen atoms.[48] a–Transition diagram of CARS processes involving the fine structure states of the oxygen atom. The $^3P_1$ state is populated thermally. b–experimental CARS spectrum. Spin-orbit Raman resonance (marked with an arrow) appears on a background of rotational transitions in vibrationally excited oxygen molecules.

its resonances (see Fig. 7, b). When the frequency difference $\omega_1 - \omega_2$ coincides with Ω_{12}, for example, (see Fig. 7, a) the resulting excitation of the magnetic dipole moment is much more effective than single-photon excitation with an infrared source. The radiative deactivation of magnetic dipole oscillations is slow (on the time scale of a second) and this transition can radiate strongly only in the presence of a third photon (in this case of frequency ω_1) which mixes in dipole moment transitions involving higher-lying electronic states.

The authors of Refs. 49, 50 studied CARS in the fine structure of halogen atoms: chlorine, prepared by dissociating molecular chlorine in a microwave discharge,[49] and bromine, prepared by photodissociation of HBr molecules.[50]

An analysis of the spectroscopic aspects of CARS in atoms has been carried out by our group.[53-55] We investigated the following transitions: $^7F_2$–$^7F_3$, $^7F_3$–$^7F_4$, $^7F_4$–$^7F_5$, $^7F_5$–$^7F_6$ in the $4f^6 6s^2$ configuration of samarium atomic vapor; $^2F^0_{5/2}$–$^2F^0_{7/2}$ in the $4f^{13}(^2F^0)6s^2$ configuration of thulium atoms; $^2P^0_{1/2}$–$^2P^0_{3/2}$ of the $6s^2(^1s)6p$ of thallium atoms. In heavy elements the excited states that are connected to the ground state by large dipole moment transitions lie quite low and are consequently quasiresonant with radiation in the visible even when the atoms are "cold". Consequently CARS processes that start from low-lying excited fine-structure states ($J = 2, 3, 4, 5$) exhibit high and approximately equal susceptibilities. The intensity of the scattered signal is accordingly large even at vapor pressures of the order of 10^{-2} Torr; the detection threshold on available equipment probably does not exceed 10^{-4} Torr.

The evolution of CARS processes at high pump intensities was studied in Refs. 56, 57. The authors investigated the spectral profile of the antiStokes signal as a function of intensity I_1 (at frequency ω_1) in atomic samarium vapor. The Raman resonance at the $^7F_4$–$^7F_5$ transition (the $^7F_4$ state was populated thermally, see Fig. 8) produces a single spectral line at 853 cm^{-1} at intensities $I_1, I_2 < 10^8$ W/cm^2 (Fig. 9). When I_1 is increased to $2 \cdot 10^9$ W/cm^2 the line splits into four components. This splitting occurs only at fairly elevated temperatures ($T > 700$ °C). Evidently, the higher-lying states of samarium are populated by the optically induced collision mechanism.[58,59] First, the $^7H^0_5$ state is populated by the quasiresonant radiation of frequency ω_1, then radiative collision processes with buffer gas atoms at $T \approx 1000$ °C effectively populate higher-lying states like $^7G^0_4$, $^7G^0_7$, and $^9F_1$. As a result "hot" lines at 846 cm^{-1} (line *1*) and 844 cm^{-1} (line *2*) appear in the CARS spectrum. Increasing the temperature of the medium or the pump intensity produces more of these lines, which eventually merge into a smooth and fairly strong background. The CARS process is effective regardless of the values of ω_1 and ω_2.

Bunkin and co-workers[60] demonstrated the feasibility of employing CARS spectroscopy on the intense optical breakdown flame in air near the surface of a tin target. These experiments yielded a fairly strong CARS signal starting from the excited fine-structure states. The authors were able to measure the polarization properties of the scattered signal and demonstrate a significant antisymmetric component in the Raman scattering tensor.

Fabelinskii and co-workers[61] studied CARS in silicon atoms prepared by photodissociation of CS_2 molecules.

We conclude this subsection by noting once more that

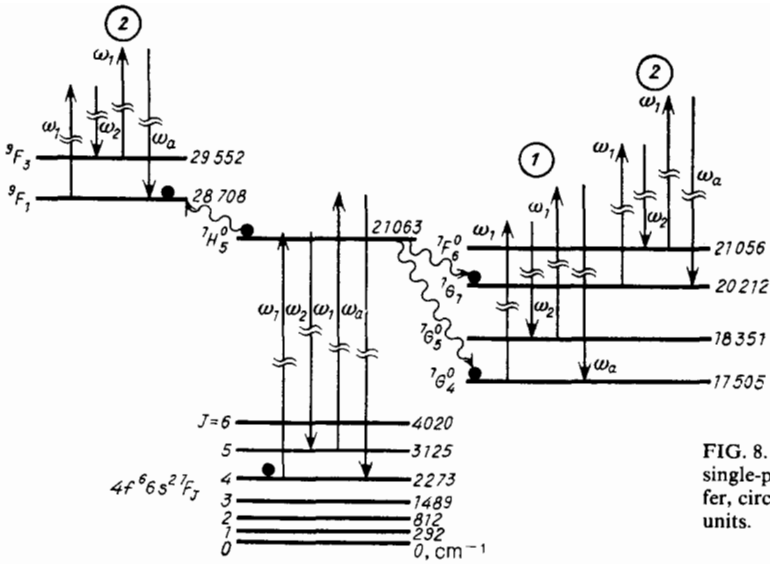

FIG. 8. Transition diagram of CARS in atomic samarium vapor near the single-photon resonance. Wavy arrows indicate collisional energy transfer, circles mark the populated states. Energies are translated into cm^{-1} units.

atomic fine-structure CARS can be employed to study the kinetics of metastable lasing states based on atomic transitions in iodine lasers, for example, or lasers based on fluorine, chlorine, or bromine atoms.

4.5. Active hyper-Raman spectroscopy in excited atoms and ions

As we mentioned earlier, the four-photon CARS process with a single-photon resonance at either the pump or the scattered signal frequency can be labeled active hyper-Raman scattering spectroscopy (AHRS) (see Fig. 1). By employing the experimental apparatus described in the preceding subsection and detecting the scattered signal at the frequency $\omega_a = 2\omega_1 - \omega_2$, a resonance of this type occurs when either ω_2 or ω_a coincides with the frequency of an allowed dipole transition in the excited atom or ion. This spectroscopic transition scheme is particularly effective precisely in highly excited media, where CARS is ineffective (since the Raman states lie close in energy and have nearly equal populations at high temperatures).

One of the first experiments of this type was described in Ref. 62 (Fig. 10). Excited atoms of iron were produced by optical breakdown at the surface of an iron target. The time delay between the breakdown and probe pulses was set at approximately 5 μs, giving the plasma time to cool and partially recombine. In this case the resonance signal is emitted at the antiStokes frequency. Since the resonance involves a dipole-active transition, spontaneous emission was observed at exactly the same frequency as the AHRS signal (see Fig. 10). In the experimental conditions of Ref. 62 the coherent scattered signal was more intense than spontaneous luminescence by 1–2 orders of magnitude. Since the coherent signal is much less intense than the pump beam, a resonance at the signal frequency is preferable to a resonance at the pump

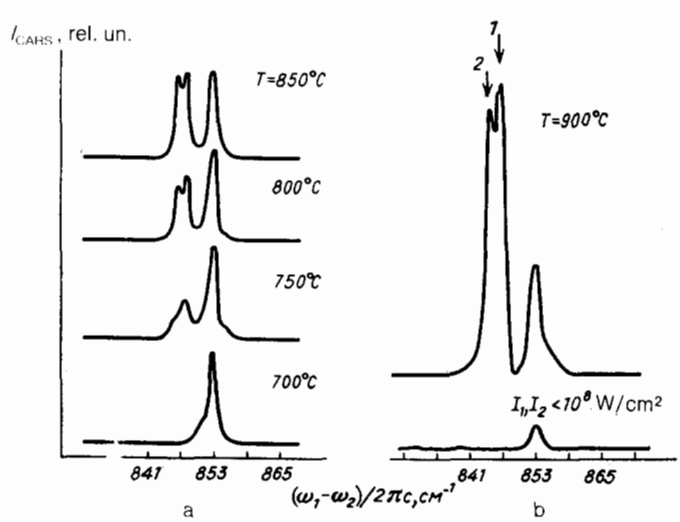

FIG. 9. CARS spectral lineshape near 853 cm^{-1} ($^7F_4$–$^7F_5$ transition) as a function of temperature (a) and pump intensity (b). Arrows mark the lines defined in the transition diagram in Fig. 8. The simultaneous effect of heating and intense pump fields establishes a quasiresonant interaction regime. The upper curves in (a) are for $I_1 = 2\cdot 10^9$ W/cm^2, $I_2 = 10^8$ W/cm^2.

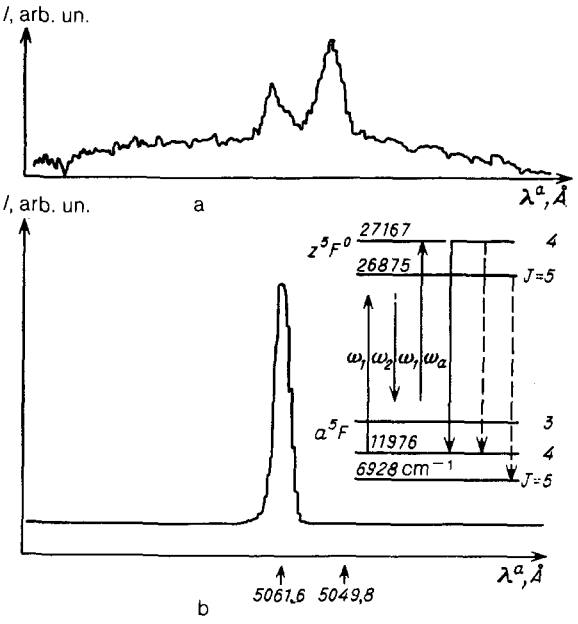

FIG. 10. Active hyper-Raman spectroscopy of excited Fe atoms in the optical breakdown flame.[62] a—Spontaneous luminescence lines of Fe atoms. b—Recorded AHRS spectrum. The insert in b shows the transition diagram, with dashed lines corresponding to spontaneous luminescence. I is the intensity of the optical signal.

frequency because the former does not saturate the transition and distort the spectroscopic data. In the experiment[62] the measured width of the AHRS resonance was less than 1 cm^{-1}, limited by the resolution of the signal acquisition system.

We should clarify why this type of four-photon resonance can be properly described as active hyper-Raman spectroscopy. This terminology and approach were introduced and developed by a number of authors.[63–67] They demonstrated that in this particular scheme the cubic susceptibility components important in AHRS can be simply expressed as:

$$\chi_{1111}=\frac{N}{24\hbar}\frac{d_{12}}{\Omega_{12}-\omega_a-i\Gamma}\left(\frac{\beta_0}{\sqrt{3}}+\frac{2\beta_2}{\sqrt{15}}\right),$$

$$\chi_{1221}=\frac{N}{24\hbar}\frac{d_{12}}{\Omega_{12}-\omega_a-i\Gamma}\left(\frac{\beta_0}{\sqrt{3}}-\frac{\beta_2}{\sqrt{15}}\right),$$

where β_i are the components of the vector part of the HRS tensor, Ω_{12} is the frequency of the resonant transition and d_{12} is the dipole moment of this transition. Consequently, the ratio of the components of the χ tensor, like the ratio of the β invariants, can be determined experimentally from polarization experiments.[7]. In particular

$$\frac{\beta_0}{\beta_2}=\frac{1+(2\,\mathrm{tg}\,\theta/\mathrm{tg}\,\varphi)}{\sqrt{5}\,[1-(\mathrm{tg}\,\theta/\mathrm{tg}\,\varphi)]},$$

where φ is the angle between the unit vectors of the pump field $\mathbf{E}$ and θ is the angle between the polarization vector of the scattered signal and the unit vector $\mathbf{e}_1$.

We note here that this type of spectroscopy can measure only the vector invariants of the HRS tensor. Complete active HRS is possible by employing a six-photon resonance (see Fig. 1). The transition under study must conform to the $|\Delta J|=3$ selection rule to avoid the cascading four-photon process. This spectroscopic scheme can be used to prepare and probe atomic octupole moments. These experiments have not been carried out to date.

Our group has reported AHRS experiments on ions excited in a low-temperature plasma.[45,68–72] The excitation was provided either by an arc[45,68] or by optical breakdown near metal surfaces. In Refs. 70–72 we measured AHRS spectra of transitions between high-lying states of atomic ions: singly ionized nitrogen, singly and doubly ionized aluminum, and singly ionized indium (Fig. 11). We also investigated the kinetics of the scattered signal.

We found that a resonance at the pump frequency usually results in a fairly broad scattering resonance, of the order of several cm^{-1}, whereas a resonance at the signal frequency produces a narrow scattering spectrum. We also found a quantitative difference between the intensity kinetics of spontaneous luminescence and coherent scattering from the same transition. The former decays rather quickly, reflecting the depopulation of the higher-lying resonant state, while the latter is proportional to the square of the population difference between the two resonating states–the coherent signal first increases and then decays slowly, as the lower resonant state (which can be metastable) is depopulated. In both cases the kinetic behavior was adequately reproduced by a simple model in which the excited states are populated by optically induced collisions. Finally, since the AHRS signal remains quite strong after the spontaneous luminescence has decayed markedly, AHRS can be utilized for spectroscopy of metastable states in a low-temperature plasma with both spatial and temporal resolution.

4.6. New methods of generating optical harmonics in excited atomic and ionized media

The idea of utilizing excited ions for resonant optical frequency conversion was first proposed by Lebedev and coworkers.[73–75] They demonstrated experimentally the feasi-

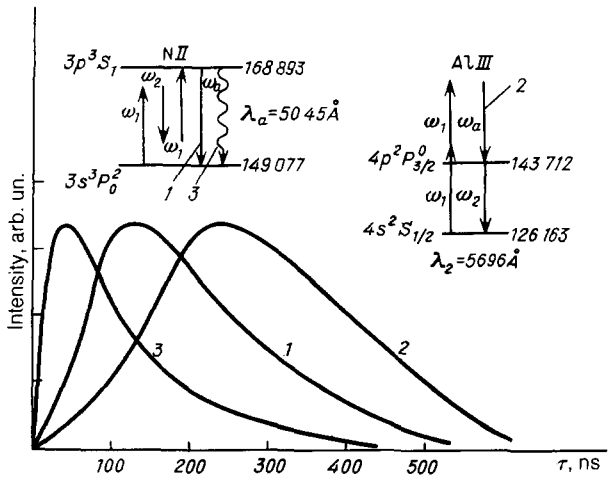

FIG. 11. Active hyper-Raman spectroscopy of atomic ions in laser plasma flames (see Refs. 70–72). The intensity kinetics of resonant AHRS signals is plotted for several resonances: NII (*1*) and AIIII (*2*) ions, together with the spontaneous luminescence of NII ions (*3*). Transition diagrams corresponding to these resonances are also shown.

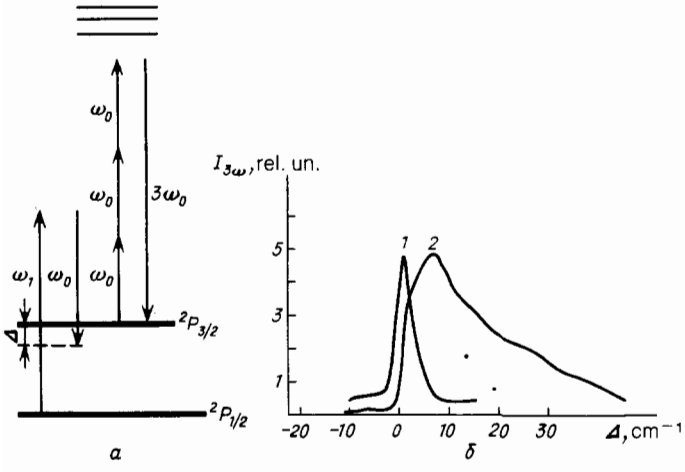

FIG. 12. Efficiency enhancement of third harmonic generation of $\lambda = 1.06$ μm radiation (frequency ω_0) in thallium vapor due to two-photon Raman excitation (TRE) of the $6P_{3/2}$ state.[77] Frequency ω_1 is tunable. a–Schematic transition diagram of the process. b–Intensity of third harmonic vs. TRE frequency detuning. In curve *2* the product of intensities $I_1 I_2$ is three orders of magnitude higher than in curve *1*.

bility of efficient third harmonic generation in magnesium atoms. The ionized medium was shown to possess new resonant frequencies better suited as light sources in the visible range.

Ganeev and co-workers[76] investigated the generation of the third harmonic of a Nd:YAG laser in a jet of excited gallium ions. Since the ion concentration was fairly low (up to 10^{18} cm^{-3}), the third harmonic signal proved rather weak (the conversion efficiency was 10^{-7}). Still, the authors estimated the cubic susceptibility of excited ions to be six orders of magnitude higher than of unexcited ones, concluding that the conversion efficiencies could become practical at higher ion concentrations.

Another two experiments[69,77] were dedicated to confirming specifically that the establishment of a quasiresonance can significantly enhance the efficiency of third harmonic generation. These experiments investigated thallium vapor at pressures of 0.1 Torr. The $6P_{3/2}$ state was selectively populated by two-photon Raman excitation (TRE)[78] that is particularly effective in atomic media[79,80] (see Fig. 12). The wavelengths employed were 1.06 μm (ω_0) and 0.58 μm (ω_1, the intended conversion frequency). As the population of the $6P_{3/2}$ state grew, the third harmonic generation efficiency increased by 3 orders of magnitude. Significantly, calculations presented in Ref. 66 indicate that this increase in efficiency is due precisely to the $\chi^{(3)}$ susceptibility enhancement and not to excitation-induced improvement in phase matching.

We should also point to other experiments[81,82] in which the resonance at the third harmonic frequency was observed with high resolution made possible by suppressing of the three-photon luminescence signal.

We conclude this subsection by restating that the quasiresonance achieved by exciting the gaseous medium allows four-photon processes to proceed at high efficiency, rendering them suitable for spectroscopic purposes as well as frequency conversion in the visible.

5. COHERENT NONLINEAR SCATTERING AND LASER FREQUENCY UP-CONVERSION IN LOW-TEMPERATURE PLASMA

5.2. *New formulation of the problem*

In this section we will examine CARS processes and harmonic generation in low-temperature plasmas produced by optical breakdown. The experiments we will discuss have a number of features that distinguish them from the nonlinear optical experiments typically performed in laser-assisted fusion research.[83–86] They are usually carried out at moderate laser pulse energies, not exceeding 200 mJ (usually 50–100 mJ). The plasma is created either by optical breakdown in gases or by breakdown near metal surfaces. Different lasers are employed for breakdown and for nonlinear optical probing, with a controlled time delay between the two laser pulses. Experimentally the time delay is set between 100 and 1000 ns, such that the plasma density does not exceed 10^{17}–10^{19} cm^{-3} and the signal frequencies are much higher than the frequency of Langmuir (longitudinal) oscillations. Consequently the plasma is almost completely transparent in the visible and/or near IR ranges. In these conditions nonlinear optical processes take place in a collinear, coherent regime and, as it turns out, with surprisingly high efficiencies.

5.1. Early experiments

The first experiments in this area were performed in our laboratory in 1981 and published in 1981–1982.[87–89] We discovered that as atmospheric air sustained optical breakdown due to focused pump pulses, the intensity of the nonresonant CARS signal increased by 1–2 orders of magnitude over the value measured in the absence of optical breakdown. This effect was confirmed in Ref. 90. Subsequently we carried out experiments on third harmonic generation with nano- and picosecond Nd:YAG laser pulses[91–93] (see also Refs. 95, 96). A simplified transition diagram of these experiments in illustrated in Fig. 13. The Nd:YAG laser was operated in the Q-switched regime (nanosecond pulses) with 100–200 mJ energy per pulse. The beam was focused onto the surface of a metal target by a cylindrical lens, creating a plasma either in vacuum or in air. In other experiments the metal target was removed and we induced breakdown in a gas by focusing with a spherical lens laser pulses propagating in the opposite direction from the probe pulse. After a time delay τ, in the 100 ns–1 μs range, nano- or picosecond pulses of another Nd:YAG laser were focused onto the plasma flame. The energy of the probe pulses did not exceed 100 mJ. Coherent third harmonic radiation propagated collinearly with the pump beam and was detected by a multichannel analyzer after passing through a polychromator. This experimental

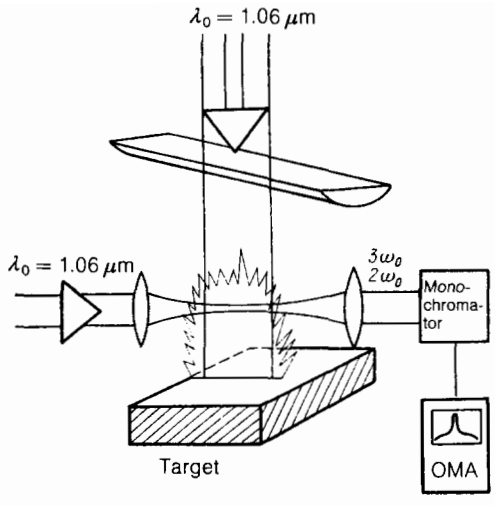

FIG. 13. Experimental arrangement for observing harmonic generation in optical breakdown plasmas.[91-93] Nd:YAG laser radiation is focused onto the surface of a metal target with a cylindrical lens. After a variable time delay τ the pump beam is focused on the plasma. The harmonics propagate collinearly with the pump beam.

arrangement differs markedly from earlier experiments by other groups.[95-97] In those experiments the authors investigated optical harmonic generation by detecting the frequency multiplication in plasmas created by the laser pulses themselves (with pulse energies reaching tens of J).

Our experiments established that whether we are studying the CARS signal or third harmonic generation, the intensity of nonresonant four-photon processes in a neutral gas increases by 1–3 and, depending on experimental conditions, even 4 orders of magnitude after laser-induced breakdown. The results on third harmonic generation in low-temperature plasmas are summarized in Table II.

The coherent scattering signal varies strongly with τ, peaking at some optimal value of the delay. We found that this optimal delay increased together with the volume occupied by the plasma. Moreover, we also detected coherent second harmonic generation, although it was significantly (by 3–5 orders of magnitude) weaker than the third harmonic signal. This can be seen as evidence that the gradient harmonic generation mechanism (due to inhomogeneities) is not the dominant one.[83]

The best results on THG efficiency enhancement were obtained recently:[93] picosecond pulses (40 ps, 40 mJ) were utilized to bring the conversion efficiency up to 3%. The third harmonic radiation was narrow-band, spatially coherent, and usable in other nonlinear optical experiments. This leads us to the practical applications of this type of optical frequency conversion. The advantages are several: the mechanism is nonresonant and hence can be used for frequency conversion of radiation tunable over a wide range; nonlinear media are universal and easily available; the technique allows for energy scaling (see below for a discussion of saturation effects). This technique can also be employed for frequency conversion in spectral ranges (UV, VUV) where nonlinear crystals are nonexistent or ineffective, for conversion of ultrashort laser pulses, etc.

5.3. Model of a classical collisional plasma

Several mechanisms can be invoked to explain the effective frequency conversion described above. First, as we have mentioned already, there is the enhancement of nonlinear susceptibilities as the excited atomic and ionic levels are populated. Second, there is the dissipative nonlinearity mechanism in collisional plasmas, developed in Refs. 98–100. This mechanism is based on the dependence of the electron-ion collision frequency ν_{ie} on electron temperature (which in a strong electromagnetic field differs from the temperature of the gas). This mechanism is important in dense, low-temperature plasmas for pulses in the nanosecond range or longer, when many collisions can occur during a single pulse.

Let us illustrate this process using a simple model.[98] Equations for electron velocity V and the temperature of the electronic plasma subsystem T_e can be written as follows:

$$\frac{dV}{dt} = \frac{e}{m} E_0 \sin(\omega t) - \nu(T_e) V,$$
$$\frac{dT_e}{dt} = \frac{2e}{3} V E_0 \sin(\omega t) - \delta\nu(T_e)(T_e - T_0); \qquad (12)$$

where E_0 is the amplitude of the external electromagnetic field (spatial dispersion is neglected); $\nu(T_e)$ is the temperature-dependent frequency of electron-ion collisions (in a fully ionized gas): $\nu(T_e) = \nu_0 (T_0/T_e)^{3/2}$, T_0 being the temperature of the gas in energy units; $\delta = m_e/m_i$.

This model was employed by Sharma[100] to calculate the THG intensity in laser radiation. In steady state the calculated conversion efficiency was rather low (10^{-5}). It was also concluded that if T_e is very different from T_0 (nonequilibrium case), conversion efficiencies of several percent are possible, but no calculations were presented in support. In steady state the derived formula for the third harmonic intensity was as follows:

TABLE II.

Ref., year	Plasma preparation	Pulse energy, mJ	Pulse duration, ps	Conversion efficiency, $W_{THG}/W_{1.06}$
[91], 1986	S *)	100	30000	10^{-10}
[91],,1986	M **)	100	30000	10^{-8}
[69], 1988	C	200	700	10^{-5}
[93], 1988	S	40	40	10^{-3}
[93], 1988	M	40	40	10^{-2}

S—Self-breakdown of atmospheric air induced by the pump of the THG process.
M—Breakdown of atmospheric gas at the surface of a metal target caused by an independent laser source.

$$P_3 = \left(\frac{3\nu_0\alpha}{16\delta\omega}\right)^2 \frac{E_0^6}{(1+\alpha E_0^2)^5},$$

where

$$\alpha = \frac{e^2E_0^2\delta}{6m(\omega^2+\nu^2)T_0}.$$

Consequently, THG efficiency saturates as the pump intensity increases . The same mechanism was investigated by others via the kinetic equation.[101,102]

Finally, we should mention nonlinear plasma mechanisms resulting from the Lorentz force[103,104] and collective plasma resonances. The former is the fundamental source of optical plasma nonlinearities. Even a noninteracting free electron feels a Lorentz force $\mathbf{F}_L \sim (e/c)\mathbf{v}\times\mathbf{H}$ in the magnetic field of the laser beam. In the dipole approximation the electron velocity $\mathbf{v}$ is proportional to the electric field: $\mathbf{v} = (e/m)\mathbf{E}$. As a result, the Lorentz force induces a nonlinear velocity component $\mathbf{v}^{(2)}$ quadratic in the amplitude of the optical field $|\mathbf{E}| \sim |\mathbf{H}|: \mathbf{v}^{(2)} \sim \mathbf{E}^2$. However, in nonrelativistic optical fields with $v/c \ll 1$ we have

$$|\mathbf{F}_L| \ll |\mathbf{F}_{dip}| = e|E|$$

and the Lorentz nonlinearity of the free electron turns out to be relatively small.

Finally, the above mechanism eventually produces nonlinear collective plasma excitations that can make nonresonant contributions to both linear and nonlinear plasma response (we will not discuss hydrodynamic mechanisms here). In a nonmagnetic plasma the dominant collective excitations are Langmuir (longitudinal) plasma oscillations at frequency $\Omega_p = (4\pi N_e e^2/m)^{1/2}$. If a biharmonic optical field containing frequencies ω_1 and ω_2 is incident on a plasma, Langmuir oscillations can be resonantly excited by the beating of the optical field components if the resonance condition $\Omega_p = \omega_1 - \omega_2$ is fulfilled. Correspondingly, just as in ordinary CARS, we find a resonant enhancement of the cubic susceptibilities for processes like four-wave mixing: $\omega_a = \omega_1 + (\omega_1 - \omega_2) = 2\omega_1 - \omega_2$. The maximum value attained by this resonant cubic susceptibility was calculated by Bloembergen and Shen back in 1966:[103]

$$\chi^{(3)} = \frac{-ie^4N\Omega_p\tau}{\omega_1^2\omega_2^2m^3c^3} = -i\frac{\Omega_p^3\tau r_0}{4\pi\omega_1^2\omega_2^2m},$$

where $r_0 = e^2/mc^2$ is the classical electron radius and τ is the energy relaxation constant of plasma oscillations. If the resonance condition were fulfilled exactly, the susceptibility could reach 10^{-17} in CGS units at $N_e \sim 10^{19}$ cm^{-3}, $\Omega_p\tau = 10^2$. However, because of plasma inhomogeneities an exact resonance cannot simultaneously occur over any reasonable interaction volume, and the observed values of $\chi^{(3)}$ should be lower by several orders of magnitude. Consequently, the average "collective" plasma nonlinearity is small and cannot give rise to observed high efficiencies of four-photon processes. Moreover, the THG transition schemes of our experiments preclude a resonance between pump frequencies in the visible and near IR and the plasma oscillation frequencies.

Finally, we note that a characteristic feature of the collective oscillation mechanism is the polarization of the CARS signal in the same direction as the pump beam of frequency ω_1.[103] We observed this polarization state in only a single experiment on atomic media: CARS in resonantly photoionized sodium vapor. Since the Na^+ ions have no quasiresonances in the visible, the plasma contribution is not masked by the signal from bound electrons.

We believe the generation of optical harmonics in the field of intense, ultra-short light pulses can be adequately described by the scattering of optical electrons from ions in the presence of an external field (see below, section 6).

5.4. Inadequacy of simple models

Various experiments[95–97] have provided evidence of the dominant role played by excited discrete states. Indeed, the CARS polarization anomaly (see Fig. 4 and section 4) can only be explained by invoking discrete states. Both the dissipative nonlinearity and electron scattering from structureless ions are essentially nonresonant mechanisms, so the $\mathbf{P}_{CARS}$ vector must lie between the $\mathbf{e}_1$ and $\mathbf{e}_2$ unit vectors (see the monograph of Ref. 7 and Ref. 110 for details). As for the Langmuir electron nonlinearity, we have already pointed out that this mechanism constrains $\mathbf{P}_{CARS}$ to be collinear with $\mathbf{e}_1$ (see, also, Ref. 103). These properties can be utilized to distinguish the nonlinearity mechanisms experimentally. In a given experimental situation, the limits of applicability of the mechanisms discussed in section 5.3 are difficult to establish–no such analysis has been attempted to date.

It appears that quantitative modeling of four-photon scattering processes in the laser breakdown flame requires a proper statistical theory that takes into account the structure of the particles comprising the flame.

The analysis is complicated by self-interacting radiation effects, such as self-focusing in a plasma. Recently, several papers addressed this effect in coherent nonlinear optical processes at fairly low gas densities and moderate incident intensities (see Refs. 14, 105–109 and references therein). For example, Sodha and co-workers[105] have shown that self-focusing in a plasma can occur at pump intensities as low as 10^8 W/cm^2. The beam contraction due to self-focusing obviously increases the pump intensity and leads to enhancement of THG efficiency by up to three orders of magnitude.[105]

6. COHERENT NONRESONANT NONLINEAR SCATTERING PROCESSES AND FREQUENCY UP-CONVERSION IN SUPER-INTENSE OPTICAL FIELDS

6.1. Super-intense optical fields: an introduction

In this section we will discuss the features of nonlinear optical processes that occur in optical fields that are comparable to or even stronger than atomic electric fields. Such processes have attracted and maintained scientific interest because of experiments on the interaction of intense, focused, sub-picosecond laser pulses with gases.[3–6] They include above-threshold ionization of atoms,[111] multiphoton stripping of atoms (MSA),[112] etc. We will concentrate on related, coherent processes that lead to multiple optical harmonic generation (MHG), which are currently the subject of much experimental and theoretical research (see published conference proceedings.[113]

In order to discuss the many experiments in this field,[3,94,116–120] consider the typical experimental apparatus and results of Ref. 114. The beam of a KrF laser (350 fs pulse duration, 20 mJ energy, $\lambda = 248$ nm) is focused on a jet of

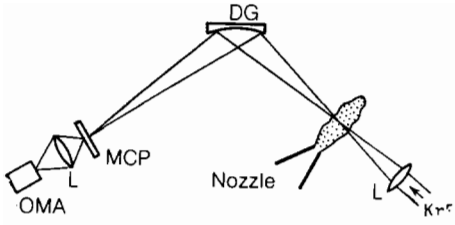

FIG. 14. Experimental arrangement used to generate multiple harmonics with focused femtosecond optical pulses. Radiation of a KrF excimer laser is focused with a lens L onto a pulsed jet of inert gas released into vacuum. DG–spherical diffraction grating; MCP–microchannel plate phosphor detector; OMA–optical multichannel analyzer.

noble gas atoms. The intensity at the focal point reaches 10^{15}–10^{16} W/cm^2 leading to multiple ionization of the atoms.[8,115] Consequently, harmonic generation occurs in a gas plasma. The optical pulse duration exceeds the Langmuir oscillation period by approximately a factor of ten. There are grounds to suppose that harmonic generation occurs via the "half-bremsstrahlung" interaction[121] of the optical electron with the "parent" ion. The harmonics are detected with a vacuum monochromator and an optical multichannel analyzer. A total of 17 harmonics were observed McPerson and coworkers[114] (see Fig. 15, a). An analogous setup allowed Ferray and coworkers[120] to observe up to 33 harmonics of a picosecond Nd:YAG laser (Fig. 15, b). The focused beam intensity in that experiment reached $3\cdot10^{13}$ W/cm^2. A characteristic feature of such experiments is the relatively slow decrease of the intensity of higher harmonics with the harmonic number–the harmonic intensities fall on a "plateau" of sorts (see Fig. 15). In Ref. 114 this plateau was explained by quasiresonant emission from transitions between states in the inner electron shells. In these experiments, as in experiments described in section 5, the harmonics were coherent and collinear with the pump beam.

We should note that according to terminology adopted at the Rochester conference,[113] a super-intense optical field is one in which the field intensity exceeds the electrostatic field at the first Bohr orbit of the hydrogen atom. In other words, the interaction between the optical electron and the super-intense field is stronger than between the electron and the ion. Since the field intensity at the first Bohr orbit is

$$E_a=\frac{e}{a_0^2}\sim 1.7\cdot10^7 \text{ CGS units};\sim 5.1\cdot10^9 \text{ V/cm}]$$

(a_0 is the Bohr radius), the corresponding "atomic" unit of optical intensity I_a is

$$I_a=\frac{c}{8\pi}E_a^2\sim 0{,}35\cdot10^{17}\text{ W/cm}^2$$

When $E>E_a$, $I>I_a$, the discrete atomic structure is suppressed. Linear and nonlinear response of the medium is then determined by continuum electronic transitions.

We should also mention, however, that in certain conditions (for instance, in ionized gaseous media) the "superintensity" threshold for excited electrons can lie much lower: in some cases Nd:YAG laser fields of only $3\cdot10^{13}$ W/cm^2 can be considered superintense (see Refs. 120, 121). The threshold can fall even lower (down to 10^{10} W/cm^2) when CO_2 lasers are employed on excited gaseous media.

In practice, super-intense optical fields interact with nonlinear dissociating atomic systems. Below we propose three very simple and instructive models, which make it possible to understand the fundamental features of harmonic excitation in these conditions.

In analyzing MHG processes in super-intense optical fields we would like to determine the following:

–what is the dependence of harmonic intensities on the pump intensity;

–does this dependence saturate and, if so, when;

–what is the maximum intensity of a given harmonic that can be generated in the super-intense field limit;

–does MHG exhibit an analog of the "peak switching" observed in above-threshold ionization (see the review by Delone and Fedorov);[111]

–what are the phase matching conditions in intense fields?

In order to determine these general properties we require simple models that permit at least a qualitative or, perhaps, a semi-quantitative analysis. Several such models have already been proposed.[9,10,122–124] Below we will consider three of these: a classical one-dimensional oscillator with a realistic (albeit nonstandard) potential; a classical fully ionized collisional plasma; and a quantum model of a hydrogen-like atom with a screened Coulomb potential.

6.2. Classical one-dimensional model

We will make use of the model already described in section 2, but now we shall treat it in the extremal field limit. As before, let $x_E = eE_0/m\omega^2$ and $x_0(t)$ be the free solution of equation (1) in section 2. In the superintense field limit x_E

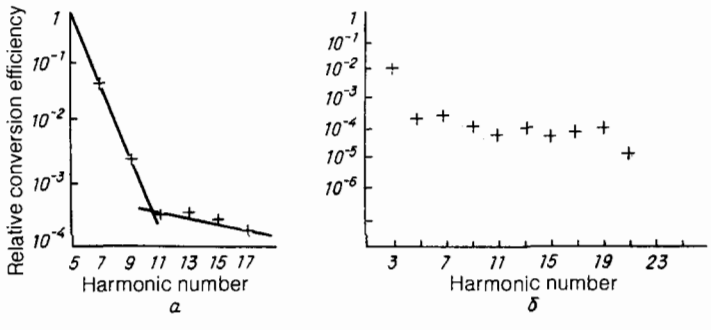

FIG. 15. Slow decay of optical harmonic intensities as a function of harmonic number in super-intense optical fields ("plateau" formation). Experimental results are shown for: a–KrF laser harmonics;[114] b–Nd:YAG laser harmonics.[120]

$\gg a$, x_0 (that is, $E \gg m\omega^2 a/e$). In this case we can find the forced solution by perturbation theory, except that now the interaction of the electron with the field will be assumed much stronger than with the ion. In the first approximation we ignore x_0 and obtain

$$x_E^{(1)} = \frac{-eE_0}{m\omega^2} \sin(\omega t);$$

In the next approximation we find the following equation

$$x_E^{''(2)} = \frac{-x_E^{(1)}}{1 + (x_E^{(1)}/a)^4} \sim \frac{A \sin \omega t}{1 + [A \sin(\omega t)]^4}, \qquad (13)$$

where A is the (dimensionless) optical field intensity: $A = eE_0/m\omega^2 a$. Equation (13) is correct whenever $A \gg 1$. It contains all the odd harmonics of the external field. In order to derive their amplitudes we can decompose (13) into a Fourier series:

$$x_E^{(2)} = \frac{a_0}{2} + \sum a_n \cos(\omega n t) + \sum b_n \sin(\omega n t). \qquad (14)$$

Clearly, only the coefficients b_n are different from zero:

$$b_n = \frac{1}{2\pi} \int_0^{2\pi} \frac{A \sin(\omega t) \sin(n\omega t)\, dt}{1 + [(A \sin(\omega t)]^4}. \qquad (15)$$

The intensity of the nth harmonic is $I_{n\omega} = a_n^2 + b_n^2 = b_n^2$. In Fig. 16 we have plotted the harmonic spectrum for several values of the dimensionless field amplitude A. As A increases more harmonics appear. The MHG spectrum exhibits a "maximum switching" that is analogous to the "peak switching" in above-threshold ionization: as A increases, the center of mass of the harmonic spectrum shifts towards higher harmonic number. Since the coefficients a_n in the Fourier series (14) are zero, all the harmonics are in phase with the external field and with each other. Consequently, we can conclude that we are dealing with a nonresonant process, just as in the case of a structureless atomic continuum. The emission field can be evaluated simply by substituting the second derivative of equation (13) as a source term into the wave equation.

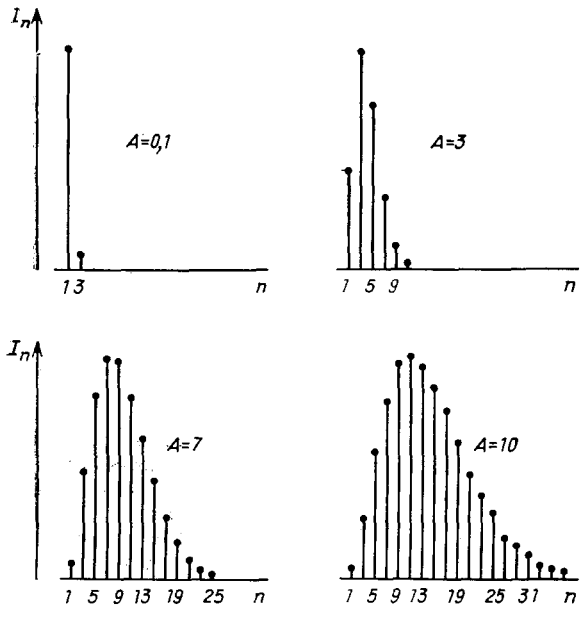

FIG. 16. Harmonic spectrum of the collisional term $x_E^{(2)}$ [see equation (13) of this review] as a function of relative perturbation amplitude A. I_n is the relative harmonic intensity; n is the harmonic number. The spectra exhibit numerous odd harmonics, as well as the "peak switching" effect.

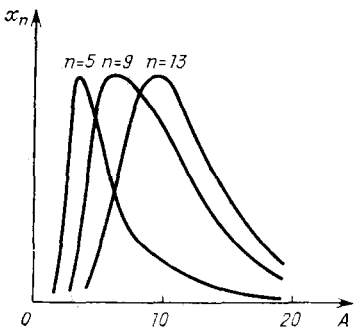

FIG. 17. Saturation of $n = 5$, 9, 13 harmonics as a function of relative amplitude A (see subsection 6.2). The initial slopes of the curves are nearly identical.

The saturation of several harmonics is illustrated in Fig. 17. The intensity of any harmonic first increases with the external field amplitude and then begins to decay. As the harmonic number increases, so does the field intensity at which the saturation sets in. This model also indicates that the total energy absorbed by the oscillator increases steadily with the pump field amplitude. The saturation mechanism is simple to understand: as the external field increases, the interaction of the electron with the ion is switched "on" and "off" more and more rapidly, becoming a series of ever-quickening pulses. Consequently, a more intense field generates higher harmonics more effectively.

The initial slopes shown in Fig. 17 are unusual for traditional perturbation theory calculations. They are practically identical regardless of harmonic number. Numerical computations show that these slopes are actually determined by the parameter n of our model, i.e., by the interaction potential (see section 2), rather than by the number of generated harmonic. This fact can be used to reconstruct the actual potential seen by the scattered optical electron. Possibly this fact also explains the unexpected slopes of the intensity peaks in the above-threshold ionization spectra measured using a CO_2 laser in the tunnel ionization regime.[125]

The higher-order approximations of perturbation theory only add some broadening without qualitatively altering the harmonic spectrum.

The above results have one more interesting consequence. Since all the optical harmonics are in phase, their direct summation narrows considerably the system response to external fields. In Fig. 18 we illustrate this phenomenon. Clearly the system response due to the electron-ion interaction becomes shorter in duration as more harmonics are present in the stimulated oscillation spectrum. For example, if we take a CO_2 laser beam sufficiently intense to generate some 100 harmonics (dimensionless amplitude A of the order of 20–30), we obtain pulses as narrow as 10^{-16} s (attosecond range). Note that these pulses (videopulses) can no longer be considered optical waves since they contain no oscillations. The effect is similar to shock wave formation in nonlinear acoustics, where the medium dispersion is small and many harmonics can be generated. In fact, short-period (30 fs) oscillations have already been observed experimen-

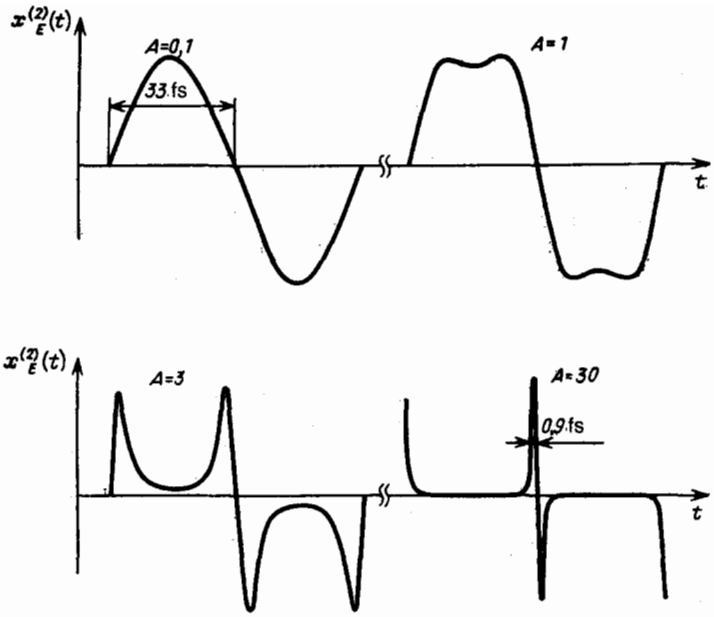

FIG. 18. Narrowing of the nonlinear response [$x_E^{(2)}$ term of equation (13)] as a function of dimensionless field amplitude A. Note the "shock wave" formation that occurs when the external perturbation oscillates at the CO_2 laser frequency. $A = 0.1$ (a), 1 (b), 3 (c), and 30 (d).

tally[126] in the interference of two well-separated Ar laser emission lines (488 and 514.5 nm). Also, De Beer and coworkers[127] observed beating in the attosecond range. Within the framework of our simple model these experiments correspond to the presence of only the first two harmonics of comparable intensity in the interference spectrum.

Obviously, a more realistic analysis of the experimental situation requires extending the above classical model to three dimensions and averaging the results over the ensemble of initial conditions. Variants of the numerical Monte-Carlo method[130–133] can be employed for this purpose.

6.3. Collisional plasma in a super-intense field

As we discussed above, sufficiently long optical pulses propagating through a dense, low-temperature plasma can be described by a simple collisional model [system of equations (12)]. Let us now place this model in a super-intense optical field. As in the preceding discussion of the one-dimensional classical model, we will apply perturbation theory by taking the interaction of plasma particles with the field to be stronger than the interaction between plasma particles. In this case the solution of (12) will have the form

$$V = V_0 + V_1 + V_2 \ldots,$$

where

$$V_0 = \frac{eF_0}{m\omega}\cos(\omega t),\quad V_1 \sim \frac{\nu(T_e)}{\omega}$$

and so forth. In the first approximation, with $V = V_0$, we have

$$\frac{dT_e}{dt} = \frac{2e}{3}\frac{eE_0^2}{m\omega}\sin(\omega t)\cos(\omega t); \tag{16}$$

This means that the average electron temperature is constant and T_e oscillates with frequency 2ω and amplitude

$$\delta T_{2\omega} = \frac{e^2E_0^2}{3m\omega}; \tag{17}$$

and $\nu(T_e)$ oscillates at the same frequency for the same reason.

In the second approximation we have

$$V_1 = -\nu(T_e)V_0 = -\nu_0 T_0^{3/2}\frac{(eE_0/m\omega)\cos(\omega t)}{[T_0 - (e^2E_0^2/6m\omega^2)\cos(2\omega T)]^{3/2}}, \tag{18}$$

i.e., as in the preceding model, all odd harmonics of the pump are present and in phase. Scattered harmonic emission is proportional to the square of the nonlinear current amplitude, i.e., to the square of the velocity amplitude. We can rewrite the above expression as

$$V_1 = \nu_0 V_0^{(0)}\frac{\cos(\omega t)}{[1 - A\cos(2\omega t)]^{3/2}}; \tag{19}$$

where

$$V_0^{(0)} = \frac{eE_0}{m\omega},\quad A = \frac{e^2E_0^2}{6m\omega^2T_0} = \frac{E_0^2}{E_p^2}.$$

here we have introduced the intensity of the "plasma field": $E_p = (6m\omega^2T_0/e^2)^{1/2}$. In this case we find that the dimensionless amplitude A is proportional to the ratio between the oscillation energy of the electron W_q and the gas temperature T_0: $A = (2/3)W_q/T_0$.

We emphasize that the above expressions are only valid if $A \gg 1$, that is if the external field is much stronger than the plasma field E_p (the latter increases as the medium is heated).

The generation of odd harmonics of an intense external field incident on a plasma was first studied by Silin,[102] who considered a more complex model.

6.4. Quantum model: hydrogen-like atom

In this model we will examine MHG processes in super-intense optical fields by considering the scattering of the optical electron of a hydrogen-like atom by its parent ion and assuming that the electron interaction with the laser field is much stronger than with the ion. Consequently the electron-

ion interaction can be treated as a perturbation.[92,93,134] This technique is quite different from the standard quantum mechanical perturbation theory calculation of nonlinear susceptibilities[38] and is much closer to the derivation of the cross-sections for multiphoton bremsstrahlung processes[135,136]–the difference being that we will concentrate on the coherent response of the medium. The estimates cited below should not be viewed as a complete theory, but rather as a first step in this direction.

The Schrödinger equation for an electron in an ionic potential that is also placed in an intense laser field $\mathbf{E}(t) = \mathbf{E}\sin\omega t$ can be written as follows:

$$i\hbar\frac{\partial\psi}{\partial t} = (H_0 + V)\psi, \tag{20}$$

where

$$H_0 = \frac{1}{2m}\left(\hbar\mathbf{k} - \frac{e}{\omega}\mathbf{E}\cos(\omega t)\right)^2$$

is the Hamiltonian of a free electron in an electromagnetic field; $V = -e^2/r$ for a Coulomb potential and $V = -(e^2/r)\exp[-\beta r]$ if Debye screening is taken into account. In both cases V is assumed to be a small perturbation.

The wavefunction of a free electron with wavevector $\mathbf{k}$ in a field $\mathbf{E}(t) = \mathbf{E}\sin\omega t$ can be written as follows:[137]

$$\varphi_k(r) = \frac{1}{(2\pi)^{3/2}}\exp\left[i\left\{\mathbf{kr} - \frac{\hbar k^2}{2m}t + \frac{e\mathbf{kE}}{m\omega^2}\sin(\omega t) - \frac{1}{4mh}\left(\frac{eE}{\omega}\right)^2\left[\frac{\sin(2\omega t)}{2\omega} + t\right]\right\}\right]. \tag{21}$$

We assume that the original, unperturbed wavefunction is described by a wavepacket

$$\psi_k^0 = N\varphi_k e^{-\alpha r},$$

that satisfies the normalization condition (N is the normalization constant):

$$\int(\psi_k^0)^*\psi_k^0 d\mathbf{r} = 1;$$

where $1 = \alpha^{-1}$ is the characteristic linear extent of electron localization determined by the parameters of the laser used to prepare this state. The average dipole moment of the system is $\langle\mathbf{d}\rangle = \langle\Psi_k^0 + \Psi_k|e\mathbf{r}|\Psi_k^0 + \Psi_k\rangle$, where Ψ_k is the correction due to the interaction with the ion. If the medium is an excited gas and the optical field is intense, the dimensions of the radiating system can be comparable to the emission wavelength and instead of the dipole moment one must average the quantity $e\mathbf{r}\exp[i\mathbf{kr}]$. The cirteria for the validity of the dipole approximation and for the "super-intensity" of the field are generally incompatible: both are satisfied for the Nd:YAG laser only in a narrow intensity range near 10^{13} W/cm^2 (see Ref. 137, p. 88). In order to simplify the calculations we will consider precisely these intensities.

The first order of perturbation theory yields the following correction Ψ_k:

$$\psi_k = \int a(\mathbf{k}')\psi_{k'}^0 d\mathbf{k}',$$

where

$$a(\mathbf{k}') = -A(\mathbf{q})\sum_{n=-\infty}^{\infty} J_n\left(-\frac{e\mathbf{qE}}{\hbar m\omega^2}\right)\frac{\exp(i\omega_{k'k}t + in\omega t)}{\hbar\omega_{k'k} + n\hbar\omega + i\cdot 0};$$

$$q = |\mathbf{q}|,\ \mathbf{q} = \mathbf{k}' - \mathbf{k},\ \omega_{k'k} = \frac{\hbar}{2m}(\mathbf{k}'^2 - \mathbf{k}^2). \tag{22}$$

In this expression $A(\mathbf{q})$ is the scattering amplitude from the spherically symmetric potential V: for the screened Coulomb potential $A(\mathbf{q}) = -4\pi e^2/(q+\beta^2)$; J_n is the Bessel function. The average correction to the dipole moment is found by averaging over the perturbed wavefunction:

$$\langle\mathbf{d}\rangle = e\int\psi_k^{0*}\mathbf{r}\psi_k d\mathbf{r} + \text{c. c.}$$

Now we can easily obtain the expression for the projection of the system dipole moment onto the field vector $\mathbf{E}$. The projected moment oscillates at frequency $n\omega$. We can average it over the initial state k:

$$d^{n\omega} = D\int\int g(\mathbf{k})A(q)G(q, E, n)\,dq\,d\mathbf{k} + \text{c. c.};\tag{23}$$

where

$$D = \frac{2^8\pi^2 i\alpha N^4}{\hbar},$$

$$G(q, E, n) = \frac{q^3}{(4\alpha^2+q^2)^3 y^2}\int_0^y\sum_{s=-\infty}^{\infty} J_s(x)J_{s-n}(x)\frac{x\,dx}{s\omega + \omega_{k'k} + i\cdot 0};$$

$$y = \frac{eqE}{\hbar m\omega^2},$$

$$A(q) = \frac{A(\mathbf{q})}{4\pi}.$$

If n is even, the components of the dipole moment projected onto $\mathbf{E}$ go to zero. The function $g(\mathbf{k})$ is the initial wavevector distribution. In some cases the function $G(q, E, n)$ can be simplified. This was done in Refs. 93, 134.

In the integral in formula (23) the effects of the external field $\mathbf{E}$ and the electron-ion interaction are separated: the function G depends only on the field, whereas $A(q)$ depends only on the interaction potential V. This formula shows explicitly that MHG processes are related to electron scattering by ions.

If the magnitude of the dipole moment is available, one can compute the emission intensity at a given frequency. For example, at the third harmonic frequency, $I_3 \sim N^2[d(3\omega)]^2 I^2$, where the factor I reflects the phase matching accuracy (see Refs. 128, 129). The problem of phase matching in plasmas and intense optical fields requires a separate discussion.

Let us also mention a theoretical study by Fedorov[138] which predicts the generation of multiple harmonics of a weak field in the presence of a second, strong field.

6.5. Phase matching in intense fields

Optical media have high dispersion because of resonances. If the resonances due to bound electrons are irrelevant (which happens in super-intense optical fields) and the density (of the plasma, in this case) is low, we should expect low dispersion. As a result, the linear susceptibility of the medium differs markedly from the low-field value. The optical electrons practically do not "see" the ions; the linear susceptibility of the initially neutral gaseous medium becomes comparable to that of a plasma. Therefore the appropriate dielectric constant is

$$\varepsilon(\omega) = 1 - \frac{\Omega_p^2}{\omega^2},$$

where Ω_p is the plasma frequency.

At gas pressures of the order of 1 Torr, plasma frequency Ω_p lies around 50 cm^{-1} (we are assuming complete single ionization). At the frequencies of the Nd:YAG laser the quantity $\varepsilon(\omega)$ is smaller than, but very close to unity: $|\varepsilon - 1| \sim 10^{-5}$. At the harmonic frequencies this deviation of ε from unity is even smaller. Still, when harmonics are generated in tightly focused beams, the deviation is large enough to reduce the generation efficiency significantly (up to several orders of magnitude). At the same time, it turns out we should take into account the existence of ions with populated discrete levels, because this improves the phase matching. The ionic contribution ε_d to the permittivity can be greater than unity (see subsection 3.1 and Fig. 3) and hence compensate the deviation of ε_p from unity.

Let us carry out some estimates for the case of third harmonic generation. The THG intensity is proportional to the square of the following expression:[128,129]

$$I(\Delta k, \xi) = \int_{-\xi}^{\xi} \frac{\exp[(1/2)\, ib\Delta k\,(\xi - \xi')]}{(1 + i\xi')^2}\, d\xi', \qquad (24)$$

$$\Delta k = k_{3\omega} - 3k_{\omega}.$$

Here we have assumed that the medium extends from $-\xi$ to ξ and

$$k_{\omega} = (\omega/c)\, n(\omega) = (\omega/c)\, (\varepsilon_p(\omega) + \varepsilon_d(\omega))^{1/2}$$

(subscripts p and d correspond to the contributions of the plasma and the discrete states respectively). It is worth emphasizing that formula (24) applies to the case of super-intense fields as well, when an alternative perturbation theory is used. For example, in the classical one-dimensional model (see subsection 6.2) the spatial phase can be taken into account by the simple substitution $\omega t \to \omega t - kx$. After expanding expression (13) in a Fourier series it turns out that, just as in standard perturbation theory, the nth harmonic has a spatial phase of nkx due to the source of the perturbation. The same is true for other models described here.

If we consider the plasma contribution only, a pump with wavelength $\lambda = 1.06$ μm and intensity $I_0 = 3 \cdot 10^{13}$ W/cm^2 (corresponding to a focused single pulse of 30 ps duration and 30 mJ energy, which satisfies the "super-intensity" criterion–see section 4) is focused on a plasma of 10^{18} cm^{-3} density, formula (24) yields I^2 of the order of 10^{-2}. If the ionic contribution to ε is also taken into account, in certain conditions I^2 can increase to become of order unity.

Estimates of third harmonic intensity from formula (23) were performed in Ref. 93 for conditions similar to the above scenario. The calculated energy conversion efficiency was 0.5% with only the plasma contribution to ε taken into account. If the dispersion is compensated by the (quasiresonant) ionic term, the efficiency can be expected to increase by an order of magnitude, in agreement with experimental results.[93] This clarifies the optimizing effect of the time delay between plasma preparation and probing: the appropriate delay sets up a quasiresonance with the discrete ionic states.

In this connection we should also mention the study by Wildenauer,[94] who investigated experimentally the generation of the 11th harmonic of the iodine laser in xenon, where the dispersion is positive. Apparently, in these experimental conditions, the beam pulling of the focused pump led to optical breakdown and the radiation interacted mainly with an excited gas (plasma) confined to a small volume. Interestingly, in the experiment the harmonic intensity changed quadratically with the gas pressure up to 0.1 atm (i.e., the phase matching did not deteriorate even at these high pressures).

It is becoming evident that multiple harmonic generation in a low-temperature plasma using techniques described in sections 5 and 6 can provide a practical means for obtaining vacuum ultraviolet and, perhaps, soft X-ray radiation. Such radiation can also be frequency-tunable.

7. CONCLUSION

Currently, research into the nonlinear optical interaction of excited gaseous media with laser beams is attracting much interest because of advances in the development and application of powerful subpicosecond laser systems. Further progress in this field will require the combined efforts of specialists in such diverse fields as quantum electronics, atomic physics, low-temperature plasma physics, quantum scattering theory, and possibly nuclear physics.

Some theoretical estimates[139] and preliminary experiments[140] indicate that atomic nuclei can begin to interact with optical beams at intensities of 10^{20} W/cm^2 and higher. Several authors[141,142] have shown that Raman scattering in the visible can include transitions between states of a compound nucleus.[143] It has been estimated,[144] that the RS cross sections of such transitions will be lower than the corresponding cross sections in molecules by only 3–5 orders of magnitude. Other light-scattering mechanisms will saturate with increasing intensity and excited nuclei will eventually begin to contribute.

Ever more intense optical fields will activate another source of optical nonlinearity neglected in this review: relativistic effects in the motion of optical electrons (particularly the energy dependence of the electron mass). The corresponding "relativistic" intensity of the optical field can be estimated by equating the oscillation energy of an electron in an electromagnetic field with the electron rest mass:

$$I_{rel} = \frac{m^2\omega^2c^3}{4\pi e^2}.$$

At frequencies ω in the visible, $I_{rel} \sim 10^{19}$ W/cm^2.

Quantum electrodynamic effects will enter into nonlinear optical processes when the optical field reaches such intensities that the work of an optical electron at the electron Compton wavelength catches up with the electron rest mass. Optical breakdown of vacuum would then become possible. Granted, the corresponding optical field intensity would be colossal: $I_{qed} \sim 10^{30}$ W/cm^2.[145,146]

Progress in this direction depends on the development of amplifiers for femtosecond laser pulses. The $I \sim 10^{19}$ W/cm^2 barrier has recently been surmounted.[113] Today one can expect the maximum attainable intensity to increase by a factor of ten every 2–3 years.

Certainly, the interaction effects due to super-intense optical fields $I > I_{qed}, I_{rel}$ will be difficult to separate from the background of the quasiresonant scattering effects described in this review. Indeed, highly excited gaseous media always contain plasma electrons and ions with populated discrete states, and an optical pulse has both spatial extent and temporal duration. Nonetheless, experimentalists are sure to find extremely interesting phenomena to study.

The authors are grateful to Prof. S. A. Akhmanov for valuable comments and discussions, to A. B. Fedorov and A. M. Zheltikov who participated in many of the discussed experiments and calculations, and to A. P. Krylova and T. A. Kuz'mina for their help with the literature.

[1]V. G. Arkhipkin and A. K. Popov, Usp. Fiz. Nauk **153**, 423 (1987) [Sov. Phys. Usp. **30**, 952 (1987)].
[2]M. C. E. Huber and R. J. Sandeman, Rep. Prog. Phys. **49**, 397 (1986).
[3]T. S. Luk, H. Pummer, K. Boyer, M. Shahidi, H. Egger, and C. K. Rhodes, Phys. Rev. Lett. **51**, 110 (1983).
[4]S. A. Akhmanov, V. M. Gordienko, M. S. Dzhidzhaev, S. V. Krayushkin, V. T. Platonenko, and V. K. Popov, Kvantovaya Elektron. **13**, 1957 (1986) [Sov. J. Quantum Electron **16**, 1291 (1986)].
[5]S. A. Akhmanov, V. A. Vysloukh, and A. S. Chirkin, *Optics of Femtosecond Laser Pulses* (in Russian), Nauka, M., 1988.
[6]J. H. Glownia, G. Arjavalingam, P. P. Sorokin, and J. E. Rothenburg, Opt. Lett. **11**, 79 (1986).
[7]S. A. Akhmanov and N. I. Koroteev, *Nonlinear Optical Methods in Light Scattering Spectroscopy* (in Russian), Nauka, M., 1981.
[8]T. S. Luk, T. Graber, H. Jara, U. Johann, K. Boyer, and C. K. Rhodes, J. Opt. Soc. Am. B **4**, 847 (1987).
[9]S. M. Gladkov and N. I. Koroteev, Lecture at IX International School on Coherent Optics, Uzhgorod (USSR), 1989.
[10]S. M. Gladkov, Proc. of XXVI Colloquim Spectroscopicium Internationale, Post Conference Volume, Sofia, 1989, p. 47.
[11]S. A. Akhmanov and R. V. Khokhlov, Nonlinear Optics, Gordon and Breach, N. Y., 1972 [Russ. original, VINITI, M., 1964].
[12]N. Bloembergen, Nonlinear Optics, Benjamin, N.Y., 1965 [Russ. transl., Mir, M., 1966].
[13]G. A. Askar'yan, Pis'ma Zh. Eksp. Teor. Fiz. **4**, 400 (1966) [JETP Lett. **4**, 270 (1966)].
[14]M. H. Key, D. A. Preston, and T. P. Donaldson, J. Phys. B **3**, L88 (1970).
[15]S. M. Gladkov, N. I. Koroteev, M. V. Rychev, and O. Shtentsel', Pis'ma Zh. Eksp. Teor. Fiz. **43**, 227 (1986) [JETP Lett. **43**, 287 (1986)].
[16]V. Sevastjanenko, Beitr. Plasmaphys. **25**, 151 (1985).
[17]H. R. Griem, Spectral Line Broadening by Plasmas, Academic Press, N. Y., 1974 [Russ. transl., G. A. Kobzev and G. V. Sholin (editors), Mir, M., 1978].
[18]C. M. Penney, J. Opt. Soc. Am. **59**, 34 (1969).
[19]G. Chen and T. J. Nee, J. Opt. Soc. Am. B **4**, 1303 (1987).
[20]L. Vriens, Opt. Commun. **11**, 396 (1974).
[21]C. N. Corliss and W. R. Bozeman, *Experimental Transition Probabilities for Spectral Lines of Seventy Elements*, NBS Monograph 53, Washington, 1962 [Russ. transl., Mir, M., 1968].
[22]W. L. Wiese, M. W. Smith, and B. M. Glennon, *Atomic Transition Probabilities, Vol. 1*, NSRDS-NBS-4, US Government Print. Office, Washington, 1966.
[23]U. Fano and J. W. Cooper, Rev. Mod. Phys. **40**, 441 (1968) [Russ. transl., L. A. Vainshtein (Ed.), Nauka, M., 1972].
[24]L. Vriens and M. Adriaansz, J. Appl. Phys. **45**, 4422 (1974).
[25]L. Vriens and M. Adriaansz, Opt. Commun. **11**, 402 (1974).
[26]S. M. Gladkov and A. M. Zheltikov, Vestnik Mosk. Univ. Ser 3, Fiz. Astron. **29**, No. 2, 51 (1988) [Moscow Univ. Phys. Bull. **43**, No. 2, 52 (1988)].
[27]R. Lange and D. Schluter, J. Quant. Spectrosc. Radiat. Transfer **33**, 237 (1985).
[28]H. Schlossberg, J. Appl. Phys. **47**, 2044 (1976).
[29]P. Braunlich, R. Hall, and P. Lambropoulos, Phys. Rev. A **5**, 1013 (1972).
[30]A. Flusberg, R. A. Weingarten, and S. R. Hartmann, Phys. Lett. A **43**, 433 (1973).
[31]L. Vriens and M. Adriaansz, J. Appl. Phys. **46**, 3146 (1975).
[32]M. Jyumonji, T. Kobayasi, and H. Inaba, Kvantovaya Élektron. **3**, 790 (1976) [Sov. J. Quantum Electron. **6**, 430 (1976)].
[33]J. C. Cummings and D. P. Aeschliman, Opt. Commun. **31**, 165 (1979).
[34]C. J. Dasch and J. H. Bechtel, Opt. Lett. **6**, 36 (1981).
[35]H. Chang, H. M. Lin, and M. H. Hwang, J. Raman Spectrosc. **15**, 205 (1984).
[36]Yu. K. Gabrielyan, G. Ts. Nersisyan, and V. O. Papanyan, Abstracts of Papers presented at XII All-Union Conf. on Coherent and Nonlinear Optics (in Russian), Izd. Mosk. Univ., M., 1985, Part 1, p. 331.
[37]S. M. Gladkov and N. I. Koroteev, Itogi Nauki i Tekhniki, Ser. "Fizicheskie Osnovy Lazernoi i Puchkovoi Tekhnologii" (Summaries of Scientific Progress, "Physical Foundations of Laser and Beam Technology" Ser.), VINITI AN SSSR, M., 1988, Vol. 2, p. 4.
[38]M. A. Yuratich and D. C. Hanna, J. Phys. B **9**, 729 (1986); N. V. Delone and V. P. Kraĭnov, *Fundamentals of Nonlinear Optics of Atomic Gases*, J. Wiley, N.Y., 1988 [Russ. original, Nauka, M., 1986].
[39]N. Bloembergen, H. Lotem, and R. T. Linch, Ind. J. Pure Appl. Sci. **16**, 151 (1978).
[40]N. L. Manakov, S. I. Marmo, and A. G. Fainshtein, Zh. Eksp. Teor. Fiz. **91**, 51 (1986) [Sov. Phys. JETP **64**, 29 (1986)].
[41]P. T. Greenland, AERE-R9986, AERE, Harwell, 1981.
[42]S. M. Gladkov, M. V. Rychev, and O. Shtentsel', Opt. Spektrosk. **61**, 6 (1986) [Opt. Spectrosc. (USSR) **61**, 4 (1986)].
[43]S. A. Akhmanov, A. F. Bunkin, S. G. Ivanov, and N. I. Koroteev, Zh. Eksp. Teor. Fiz. **74**, 1272 (1978) [Sov. Phys. JETP **47**, 667 (1978)].
[44]J. A. Koningstein, *Introduction to the Theory of Raman Effect*, Reidel, Dordrecht, Holland, 1972 [Russ. transl., Mir, M., 1975].
[45]S. M. Gladkov, N. I. Koroteev, M. V. Rychev, V. N. Sergeev and A. B. Fedorov, Izv. Akad. Nauk SSSR, Ser. Fiz. **50**, 1139 (1988) [Bull. Acad. Sci. USSR, Phys. Ser. **50**, No. 6, 92 (1986)].
[46]S. M. Gladkov and N. I. Koroteev, *Lasers and Their Applications: Proc. of 4th Summer School on Quantum Electronics*, A. Y. Spasov (editor), Sunny Beach, Bulgaria, 1986, World Scientific, Singapore, 1987, p. 286.
[47]S. M. Gladkov, in: *Lasers in Atomic, Molecular, and Nuclear Physics: Proc. of 4th Intern. School on Laser Applications in Atomic, Molecular, and Nuclear Physics*, V. S. Letokhov (editor), Vilnius, USSR, 1987, World Scientific, Singapore, 1989, p. 366.
[48]R. E. Teets and J. H. Bechtel, Opt. Lett. **6**, 458 (1981).
[49]D. S. Moore, Chem. Phys. Lett. **89**, 131 (1982).
[50]IXC. R. Quick and D. S. Moore, J. Chem. Phys. **79**, 759 (1983).
[51]Wang Ahlian and Zou Yinghua, Chin. Phys. **3**, 1004 (1983).
[52]Han Xiaofeng, Zhenguo Lu, and Zuguang Ma, Opt. Commun. **67**, 383 (1988).
[53]E. B. Aleksandrov, S. A. Akhmanov, S. M. Gladkov, N. I. Koroteev, V. N. Kulyasov, and A. B. Fedorov, Opt. Spektrosk. **58**, 721 (1985) [Opt. Spectrosc. (USSR) **58**, 439 (1985)].
[54]S. M. Gladkov, N. I. Koroteev, A. B. Fedorov, E. B. Aleksandrov, and V. N. Kulyasov, Abstracts of Papers presented at XII All-Union Conf. on Coherent and Nonlinear Optics (in Russian), Izd. M. Univ., M., 1985, Part 1, p. 252.
[55]E. B. Aleksandrov, S. A. Akhmanov, S. M. Gladkov, N. I. Koroteev, V. N. Kulyasov, and A. B. Fedorov, Izv. Akad. Nauk SSSR, Ser. Fiz. **51**, 224 (1987) [Bull. Acad. Sci. USSR, Phys. Ser. **51**, No. 2, 15 (1981)].
[56]S. M. Gladkov, A. M. Zheltikov, and O. S. Il'yasov, Abstracts of Papers presented at XX Conf. on Spectroscopy (In Russian), Kiev, 1988, Part 1, p. 101.
[57]S. M. Gladkov, O. S. Il'yasov, and I. A. Sychev, Opt. Spektrosk. **66**, 467 (1989) [Opt. Spectrosc. (USSR) **66**, 271 (1989)].
[58]A. M. Bonch-Bruevich, S. G. Prizhibel'skiĭ, V. V. Khromov, *et al.*, Izv. Akad. Nauk SSSR, Ser. Fiz. **48**, 587 (1984) [Bull. Acad. Sci. USSR, Phys. Ser. **48**, No. 3, 171 (1984)].
[59]D. B. Lidow, R. W. Falcone, J. F. Young, and S. E. Harris, Phys. Rev. Lett. **36**, 462 (1976).
[60]S. B. Bunkin, S. M. Gladkov, A. M. Zheltikov, N. I. Koroteev, V. B. Morozov, M. V. Rychev, and A. B. Fedorov, Opt. Spektrosk **66**, 1182 (1989) [Opt. Spectrosc. (USSR) **66**, 690 (1989)].
[61]V. I. Fabelinski, G. Marowsky, V. V. Smirnov, and J. Arnold, Chem. Phys. Lett. **156**, 159 (1989).
[62]S. M. Gladkov, N. I. Koroteev, M. V. Rychev, and A. B. Fedorov, Kvantovaya Elektron. **14**, 1086 (1987) [Sov. J. Quantum Electron. **17**, 687 (1987)].
[63]Yu. A. Il'inskiĭ and V. D. Taranukhin, Kvantovaya Élektron. No. 8, 1799 (1974) [Sov. J. Quantum Electron. **4**, 997 (1974–75)].
[64]Yu. A. Il'inskii and V. D. Taranukhin, Zh. Eksp. Teor. Fiz. **69**, 833 (1975) [Sov. Phys. JETP **42**, 425 (1975)].
[65]S. A. Akhmanov, A. I. Kovrigin, V. I. Kuznetsov, S. M. Pershin, and A. I. Kholodnykh, Kvantovaya Elektron. **5**, 189 (1978) [Sov. J. Quantum Electron. **8**, 113 (1978)].
[66]L. S. Aslanyan, *Abstract of Dissertation for Candidate of Physicomathematical Sciences Degree* (in Russian), Moscow State University, M., 1980.
[67]L. S. Aslanyan and N. I. Koroteev, Kvantovaya Élektron. **6**, 942 (1979) [Sov. J. Quantum Electron. **9**, 557 (1979)].
[68]S. M. Gladkov, N. I. Koroteev, M. V. Rychev, V. N. Sergeev, and A. B. Fedotov, Pis'ma Zh. Tekh. Fiz. **12**, 728 (1986) [Sov. Tech. Phys. Lett. **12**, 300 (1986)].
[69]S. M. Gladkov, A. M. Zheltikov, N. I. Koroteev, V. B. Morozov, M. V. Rychev, V. G. Tunkin, and A. B. Fedotov, Izv. Akad. Nauk SSSR, Ser. Fiz. **52**, 217 (1988) [Bull. Acad. Sci. USSR, Phys. Ser. **52**, No. 2, 7 (1988)].
[70]S. M. Gladkov, A. M. Zheltikov, N. I. Koroteev, I. S. Koleva, and A. B.

Fedotov, Pis'ma Zh. Tekh. Fiz. **15**, 24 (1989) [Sov. Tech. Phys. Lett. **15**, 10 (1989)].
[71]S. Gladkov, A. Jeltikov (Zheltikov), N. Koroteev, I. Koleva, and A. Fedotov, Proc. of XXVI Colloquim Spectroscopicium Internationale, Sofia, 1989, Vol. 1 (A-L), p. 186.
[72]S. M. Gladkov, A. M. Zheltikov, N. I. Koroteev, and A. B. Fedotov, Abstracts (In Russian) of Reports presented at II All-Union Seminar "Physics of Rapid Plasma Processes", Grodno, Belorussian SSR, 1989, p. 68.
[73]V. V. Lebedev, V. M. Plyasulya, B. I. Troshin, and V. P. Chebotaev, in: *Frequency-Tunable Lasers* (in Russian), ITF SO AN SSSR, Novosibirsk, 1984, p. 141.
[74]V. V. Lebedev, V. M. Plyasulya, B. I. Troshin, and V. P. Chebotaev, Kvantovaya Élektron. **12**, 866 (1985) [Sov. J. Quantum Electron. **15**, 568 (1985)].
[75]V. V. Lebedev and V. M. Plyasulya, Kvantovaya Élektron. **15**, 127 (1988) [Sov. J. Quantum Electron. **18**, 82 (1988)].
[76]R. A. Ganeev, V. V. Gorbushin, I. A. Kulagin, T. Usmanov, and S. T. Khudaiberdiev, Pis'ma Zh. Tekh. Fiz. **15**, 11 (1989) [Sov. Tech. Phys. Lett. **15**, 4 (1989)].
[77]F. Sh. Ganimakhov, N. I. Koroteev, V. B. Morozov, M. V. Rychev, S. V. Sarkisov, and V. G. Dunkin, Pis'ma Zh. Tekh. Fiz. **14**, 1570 (1988) [Sov. Tech. Phys. Lett. **14**, 684 (1988)].
[78]A. M. Brodnikovskiĭ, S. M. Gladkov, M. G. Karimov, and N. I. Koroteev Zh. Eksp. Teor. Fiz. **84**, 1664 (1983) [Sov. Phys. JETP **57**, 971 (1983)].
[79]S. M. Gladkov, A. M. Zheltikov, O. S. Il'yasov, N. I. Koroteev, and V. N. Kulyasov, Abstracts of Papers presented at XIII All-Union Conference on Coherent and Nonlinear Optics (in Russian), Minsk, 1988.
[80]S. M. Gladkov, A. M. Zheltikov, O. S. Il'yasov, N. I. Koroteev, and V. N. Kulyasov, Opt. Spektrosk **65**, 249 (1988) [Opt. Spectrosc. (USSR) **65**, 149 (1988)].
[81]M. G. Payne, W. R. Garrett, and W. R. Ferrell, Phys. Rev. A **34**, 1143 (1986).
[82]M. G. Payne, W. R. Garrett, W. R. Ferrell, and J. C. Miller, Phys. Rev. A **34**, 1165 (1986).
[83]N. G. Basov, V. Yu. Bychenkov, O. N. Krokhin, M. V. Osipov, A. A. Rupasov, V. P. Silin, G. V. Sklizkov, A. N. Starodub, V. T. Tikhonchuk, and A. S. Shikanov, Kvantovaya Élektron. **6**, 1829 (1979) [Sov. J. Quantum Electron. **9**, 1081 (1979)]; D. S. Bethune, Phys. Rev. A **23**, 3139 (1981).
[84]J. L. Bobin, Phys. Rep. **122**, 173 (1985).
[85]M. H. Key and R. J. Hutcheon, Adv. Atom. Molec. Phys. **16**, 201 (1980).
[86]L. M. Goldman, W. Seka, K. Tanaka, R. Short, and A. Simon, Can. J. Phys. **64**, 969 (1986).
[87]N. A. Bez'yazychnyĭ, S. M. Gladkov, V. N. Zadkov, M. G. Karimov, and N. I. Koroteev, Abstracts of Papers presented at V All-Union Conf. on Nonresonant Interactions of Optical Radiation with Matter (in Russian), GOI, L., 1981, p. 375.
[88]A. M. Brodnikovskiĭ, S. M. Gladkov, V. N. Zadkov, M. G. Karimov, and N. I. Koroteev, Pis'ma Zh. Tekh. Fiz. **8**, 497 (1982) [Sov. Tech. Phys. Lett. **8**, 216 (1982)].
[89]S. M. Gladkov and N. I. Koroteev, Abstracts of Papers presented at VI All-Union Conf. on Interaction of Optical Radiation with Matter (in Russian), Palanga, Lithuanian SSR, 1984, p. 40.
[90]E. J. Beiting, Appl. Opt. **24**, 3010 (1985).
[91]S. M. Gladkov, N. I. Koroteev, M. V. Rychev, and A. B. Fedotov, Pis'ma Zh. Tekh. Fiz. **12**, 1272 (1986) [Sov. Tech. Phys. Lett. **12**, 527 (1986)].
[92]S. M. Gladkov and A. M. Zheltikov, Abstracts of Papers presented at VII All-Union Conf. on Interaction of Optical Radiation with Matter (in Russian), GOI, L., 1988, p. 221.
[93]S. M. Gladkov, N. I. Koroteev, A. M. Zheltikov, and A. B. Fedotov, Pis'ma Zh. Tekh. Fiz. **14**, 1399 (1988) [Sov. Tech. Phys. Lett. **19**, 610 (1988)].
[94]J. Wildenauer, J. Appl. Phys. **62**, 41 (1987).
[95]N. H. Burnett, H. A. Baldis, M. C. Richardson, and G. D. Enright, Appl. Phys. Lett. **31**, 172 (1977).
[96]E. A. McLean, J. A. Stamper, B. H. Ripin, H. R. Griem, J. M. McMahon, and G. D. Bodner, Appl. Phys. Lett. **31**, 825 (1977).
[97]R. L. Garman, C. K. Rhodes, and C. K. Benjamin, Phys. Rev. A **24**, 2649 (1981).
[98]V. L. Ginzburg, *Propagation of Electromagnetic Waves in Plasmas*, Pergamon Press, Oxford, 1970 [Russ. original Fizmatgiz, M., 1960].
[99]V. P. Silin, *High-Power Parametric Interactions with Plasmas* (in Russian), Nauka, M., 1973.
[100]A. K. Sharma, J. Appl. Phys. **55**, 690 (1984).
[101]P. Rosen, Phys. Fluids **4**, 341 (1961).
[102]V. P. Silin, Zh. Eksp. Teor. Fiz. **47**, 2254 (1964) [Sov. Phys. JETP **20**, 1510 (1965)].
[103]N. Bloembergen and Y. R. Shen, Phys. Rev. **141**, 298 (1966).
[104]E. S. Sarachick and G. T. Schappert, Phys. Rev. D **1**, 2738 (1970).
[105]M. S. Sodha, R. K. Khanna, and V. K. Tripathi, Phys. Rev. A **12**, 219 (1975).
[106]C. E. Max, Phys. Fluids **19**, 74 (1976).
[107]D. Batani, F. Biaconi, A. Giulietti, D. Giulietti, and L. Nocera, Opt. Commun. **70**, 38 (1989).
[108]D. Giulietti, G. P. Banfi, I. Deha, A. Giulietti, M. Lucchesi, L. Nocera, C. Z. Zun, Laser Part. Beams **6**, 141 (1988).
[109]C. Joshi, C. E. Clayton, K. Marsh, Y. Sakawa, and R. L. Savager, Opt. Commun. **70**, 44 (1989).
[110]S. M. Gladkov, Vestnik Mosk. Univ., Ser. 3, Fiz. Astron. **30**, No. 2, 60 (1989) [Moscow Univ. Phys. Bull. **44**, No. 2 (1989)].
[111]N. B. Delone and M. V. Fedorov, Usp. Fiz. Nauk **158**, 215 (1989) [Sov. Phys. Usp. **32**, 500 (1989)].
[112]M. Crance, Phys. Rep. **144**, 118 (1987).
[113]J. H. Eberly and W. G. Greewood (editors), Conference on Super-Intense Laser-Atom Physics, University of Rochester, Rochester, U.S., 1989.
[114]A. McPherson, G. Gibson, H. Jara, U. Johann, I. A. McIntyre, K. Boyer, and C. K. Rhodes, J. Opt. Soc. Am. B **4**, 595 (1987).
[115]P. Lambropoulos, Phys. Rev. Lett. **55**, 2141 (1985).
[116]J. Bokor, P. H. Bucksbaum, and R. R. Freeman, Opt. Lett. **8**, 217 (1983).
[117]T. S. Luk, A. McPerson, H. Jara, U. Johann, I. A. McIntyre, A. P. Schwarzenbach, and C. K. Rhodes, in: *Ultrafast Phenomena V*, G. R. Fleming and A. E. Siegman (editors), Springer-Verlag, Berlin, Heidelberg, New York, Tokyo, 1986, p. GP-6.
[118]U. Johann, T. S. Luk, I. A. McIntyre, A. McPerson, A. P. Schwarzenbach, K. Boyer, and C. K. Rhodes, in: *Short Wavelength Coherent Radiation: Generation and Applications*. Topical Meeting, Monterey, California, March 24–26, 1986, D. A. Attwood and J. Bokor (editors), Am. Inst. Phys., N. Y., 1986, p. 157.
[119]U. Johann, T. S. Luk, I. A. McIntyre, A. McPerson, A. P. Schwarzenbach, K. Boyer, and C. K. Rhodes, in: *Short Wavelength Coherent Radiation: Generation and Applications*. Topical Meeting, Monterey California, March 24–26, 1986, D. A. Attwood and J. Bokor (editors), Am. Inst. Phys., N. Y., 1986, p. 202.
[120]M. Ferray, A. L'Huillier, X. F. Li, L. A. Lompre, G. Mainfray, and C. Manus, J. Phys. B **21**, L31 (1988).
[121]J. Kupersztych, Europhys. Lett. **4**, 23 (1987).
[122]J. H. Eberly, Q. Su, and J. Javanainen, Izv. Akad. Nauk SSSR, Ser. Fiz. **53**, 1101 (1989) [Bull. Acad. Sci. USSR, Phys. Ser. **53**, No. 6 (1989)].
[123]J. H. Eberly, Q. Su, and J. Javanainen, U. Opt. Soc. Am. B **6**, 1289 (1989).
[124]J. H. Eberly, Q. Su, and J. Javanainen, Phys. Rev. Lett. **62**, 881 (1989).
[125]S. L. Chin, W. Xiong, and P. Lavigne, J. Opt. Soc. Am. B **4**, 853 (1987).
[126]Z. Y. Ou, E. C. Gage, B. E. Magill, and L. Mandel, Opt. Commun. **69**, 1 (1988).
[127]D. De Beer, E. Usadi, and S. R. Hartmann, Phys. Rev. Lett. **60**, 1262 (1988).
[128]K. B. Miles and S. E. Harris, IEEE J. Quantum Electron. **QE-9**, 470 (1973).
[129]J. Reintjes, *Nonlinear Optical Processes in Liquids and Gases*, Academic Press, Orlando, 1984 [Russ. transl., Mir, M., 1987].
[130]R. Abrines and I. C. Percival, Proc. Phys. Soc. London **88**, 861 (1966).
[131]G. R. Kyrala, J. Opt. Soc. Am. B **4**, 731 (1987).
[132]J. Grochmalicki, J. Mostowski, and M. Trippenbach, J. Phys. B **21**, 1673 (1988).
[133]J. S. Cohen, Phys. Rev. A **26**, 3008 (1982).
[134]S. A. Akhmanov, S. M. Gladkov, N. I. Koroteev, and A. M. Zheltikov, Preprint No. 5, Physics Dept. Moscow Univ., M., 1988.
[135]F. V. Bunkin and M. F. Fedorov, Zh. Eksp. Teor. Fiz. **49**, 1215 (1965) [Sov. Phys. JETP **22**, 844 (1966)].
[136]N. M. Kroll and K. M. Watson, Phys. Rev. A **8**, 804 (1973).
[137]P. V. Elyutin, *Theoretical Foundations of Quantum Radiophysics* (in Russian), Izd. M. Univ., M., 1982.
[138]M. V. Fedorov, Zh. Eksp. Teor. Fiz. **69**, 849 (1975) [Sov. Phys. JETP **41**, 601 (1975)].
[139]K. Boyer, T. S. Luk, and C. K. Rhodes, Phys. Rev. Lett. **60**, 557 (1988).
[140]L. C. Biedenharn, C. A. Rinker, and J. C. Solem, Bull. Am. Phys. Soc. **32**, 1043 (1987).
[141]D. F. Zaretskiĭ and V. V. Lomonosov, Yad. Fiz. **41**, 655 (1985) [Sov. J. Nucl. Phys. **41**, 417 (1985)].
[142]S. M. Gladkov, in: *Lasers in Atomic, Molecular, and Nuclear Physics: Proc. of 4th Intern. School on Laser Applications in Atomic, Molecular, and Nuclear Physics* (In Russian), V. S. Letokhov (editor), Vilnius, USSR, 1987, World Scientific, Singapore, 1989, p. 47.
[143]L. B. Pikel'ner, Yu. P. Popov, and É. I. Sharapov, Usp. Fiz. Nauk **137**,

39 (1982) [Sov. Phys. Usp. 25, 298 (1982)].
[144]P. Golovinskiĭ, Proc. of IX Intern. School on Coherent Optics, (in Russian), Uzhgorod, Ukrainian SSR, 1989, p. 7.
[145]V. O. Papanyan and V. I. Ritus, Tr. Fiz. Inst. Akad. Nauk SSSR **168**, 120, 141 (1986) [Proc. (Tr.) P. N. Lebedev Phys. Inst., Acad. Sci. USSR **168** (1986)].
[146]A. A. Grib, S. G. Mamaev, and V. M. Mostapenko, *Vacuum Quantum Effects in Intense Fields* (in Russian), Énergoizdat, M., 1988.

Translated by A. Zaslavsky